

Computational Modeling of Avascular Femoral Necrosis using Finite Element Analysis



By

Sidra Yasmin Malik

NUST201463260MRCMS64014F

Supervisor

Dr. Zartasha Mustansar

Masters of Science in Computational Sciences and
Engineering

**Research Center for Modeling and Simulation National
University of Sciences and Technology Islamabad,
Pakistan**

August 2018

Computational Modeling of Avascular Femoral Necrosis using Finite Element Analysis



By

Sidra Yasmin Malik

NUST201463260MRCMS64014F

Supervisor

Dr. Zartasha Mustansar

A thesis submitted in partial fulfillment of the requirements for Master
of Science In Computational Sciences and Engineering (CS & E)

Research Center for Modeling and Simulation
National University of Sciences and Technology

August 2018

THESIS ACCEPTANCE CERTIFICATE

Certified that final copy of MS/MPhil thesis written by Miss. **Sidra Yasmin Malik** Registration No. **NUST201463260MRCMS64014F** of **RCMS** has been vetted by undersigned, found complete in all aspects as per NUST Statues/Regulations, is free of plagiarism, errors and mistakes and is accepted as partial fulfillment for award of MS/MPhil degree. It is further certified that necessary amendments as pointed out by GEC members of the scholar have also been incorporated in the said thesis.

Signature with stamp: _____

Name of Supervisor: Dr.Zartasha Mustansar

Date: _____

Signature of HoD with stamp: _____

Date: _____

Countersign by

Signature (Dean/Principle): _____

Date _____

Approval

It is certified that the contents and form of the thesis entitled “**Computational Modeling of Avascular Femoral Necrosis using Finite Element Analysis**” submitted by **Sidra Yasmin Malik** have been found satisfactory for the requirement of the degree.

Advisor: **Dr. Zartasha Mustansar**

Signature: _____

Date: _____

Committee Member 1: **Dr. Salma Sherbaz**

Signature: _____

Date: _____

Committee Member 2: **Dr. Rehan Zafar Paracha**

Signature: _____

Date: _____

Committee Member 3: **Dr. Ammar Mushtaq**

Signature: _____

Date: _____

Dedication

“To My Loving Father and Mother”

STATEMENT OF ORIGINALITY

I hereby declare that this submission is my own work and to the best of my knowledge it contains no materials previously published or written by other person, nor material which to a substantial extent has been accepted for the award of any degree or diploma at RCMS, NUST or at any other educational institute, except where due acknowledgement has been made in the thesis. Any contribution made to the research by others, with whom I have worked at RCMS, NUST or elsewhere, is explicitly acknowledged in the thesis. I also declare that the intellectual content of this thesis is the product of my own work, except for the assistance from others in the project's design and conception or in style, presentation and linguistics which has been acknowledged.

Author Name: **Sidra Yasmin Malik**

Signature: _____

Acknowledgments

First of all, I would like to express my humble gratitude to Allah Almighty for his countless blessing. He provided me with the knowledge and courage to complete this research.

Then, I would like to pay bundle of regards to my supervisor Dr. Zartasha Mustansar for her patience, motivation and immense knowledge. As my teacher and mentor, she has taught me more than I could ever give her credit for here. Without her support, I would not be able to complete this project.

Beside my supervisor, I would like to thank my GEC members, Dr. Salma Sherbaz, Dr. Rehan Zafar Paracha and Dr. Ammar Mushtaq for their valuable suggestion and input on the thesis.

No body has been more important to me in the pursuit of this project than my family. I would like to pay my profound gratitude to my loving Father and Mother for their never ending love, care and support. I believe that it is their confidence in me that led me to complete this project.

I am also in debt to my loving brothers Yasir Junaid Malik and Waqas Ahmed Malik and sister Ateeqa Malik for their support and confidence in me.

I would like to pay bundle of thanks to my friends especially to Saima Yaqub and Slaman Saghir for providing me help and support in my thick and thin. I'm much obliged to have friends like these. I am also grateful to all of those with whom I have had the pleasure to work during this project.

In the last, I would like to thank RCMS for providing the flat form and opportunity to complete this research.

Sidra Yasmin Malik

Content

List of Abbreviations.....	xi
List of Figure.....	xii
List of Tables.....	xv
Abstract.....	xvi
Chapter 1: Introduction.....	1
Overview.....	1
1.1 Motivation.....	1
1.2 Research Question.....	2
1.3 Research Objectives.....	2
1.4 Research Contribution.....	3
1.5 Thesis layout.....	3
Chapter 2: Literature Review.....	5
Overview.....	5
2.1 Basic Science	5
2.1.1 What is Bone?.....	5
2.1.2 Anatomy Hip.....	8
2.1.3 Anatomy of Femur.....	9
2.2 Avascular Femoral Necrosis.....	10
2.2.1 Occurrence of AVN.....	11
2.2.2 Etiology of AVN.....	13
i. Traumatic.....	13
ii. Non-traumatic.....	14
iii. Idiopathic.....	15
2.2.3 Stages of AVN.....	16
2.2.4 Diagnosis.....	21
2.2.5 Diagnostic Techniques.....	22

2.2.6 Staging and Classification of AVN.....	22
2.2.7 Treatment.....	25
i. Non-Conservative Treatment.....	25
ii. Conservative Treatment.....	26
2.3 Finite Element Method and AVN.....	26
2.3.1 Introduction to FEM.....	26
2.3.2 FEM and AVN.....	28
2.3.3 AVN Models.....	30
2.4 Missing Links in Literature.....	32
Chapter 3: Methodology.....	33
Overview.....	33
3.1 Work Flow.....	34
3.2 Image Acquisition.....	35
3.3 Image Segmentation.....	36
3.4 3-Matic For Mesh Generation.....	41
3.5 Healthy and Diseased Models.....	42
3.5.1 Diseased Model Generation.....	43
3.6 Numerical Modeling Using FEA.....	46
3.6.1 Boundary Conditions.....	46
3.6.2 Convergence Analysis.....	48
3.7 Comparisons of Results.....	49
Chapter 4: Results.....	50
Overview.....	50
4.1 Results from Scanning.....	50
4.2 Results from Image Processing.....	51
4.2.1 3-Matic Results.....	54

4.2.2 Results For Healthy Models.....	55
4.2.3 Results For AVN Models.....	55
4.3 Results From Finite Element Analysis.....	57
4.3.1 Convergence Analysis.....	57
4.3.2 Results From Healthy Models.....	59
4.3.3 Results of AVN Models	62
4.3.4 Effect of Weight on AVN Model.....	68
4.4 Comparisons of Results.....	69
4.5 Comparisons of results of Healthy and AVN Models.....	71
Chapter 5: Discussion.....	73
Future Work.....	75
References.....	76

List of Abbreviations

2D	Two-Dimensional
3D	Three-Dimensional
AVN	Avascular Necrosis
BC	Boundary Condition
CT	Computed Tomography
MRI	Magnetic Resonance Imaging
FEM	Finite Element Method
FEA	Finite Element Analysis
THR	Total Hip Replacement
ROI	Region of Interest
ARCO	Association Research Circulation Osseous
JOP	Japanese Orthopedic Association
DICOM	Digital Imaging and Communication in Medicine
CAE	Computer Aided Engineering

List of Figures

Figure 2.1 Hierarchical Origanization of Bone	8
Figure 2.2 Anatomy of Hip Joint	9
Figure 2.3 Anatomy of Femur Bone	10
Figure 2.4 Series of events for the onset of AVN	18
Figure 2.5 Micro-angiographic Study of femur head with AVN	19
Figure 2.6 (a) Radiograph of Early Stage of AVN	20
(b) MRI of Stage O of AVN	
Figure 2.7 Representation of necrotic and sclerotic area	20
Figure 2.8 (a) Femur Head showing area of hyperlucency with arrows	21
(b) Femur head representing subchodral fracture with crescent Sign	
Figure 2.9 Steps of Finite Element Analysis	27
Figure 3.1 Project Flow Diagram	34
Figure 3.2 Process Flow Diagram of Mimics Innovation Suite 19	36
Figure 3.3 Pre-defined Threshold Values, Views; A:Coronal view,B: Axial view,C: Sagittal view	37
Figure 3.4 Cropped <i>ROI</i> 2D, Views; A:Coronal view,B: Axial view, C: Sagittal view	38
Figure 3.5 Right Femur attached with Plevis, Views; A:Coronal view, B: Axial view,C: Sagittal view	38
Figure 3.6 (a) Split Mask Function 2D,Pink colour: Femur Bone, Purple colour: Pelvis,Views; A:Coronal view,B: Axial view,C:Sagittal view	39 40

<p>(b) Femur bone after Split Mask Function 2D, Views; A:Coronal view,B: Axial view,C: Sagittal view</p>	
<p>(c) Pelvis after Split Mask Function 2D, Views; A:Coronal view, B: Axial view,C: Sagittal view</p>	
<p>Figure 3.7 (a) Cortical Bone 2D, Views; A:Coronal view,B: Axial view C: Sagittal view</p>	40
<p>(b) Cancellous Bone 2D, Views; A:Coronal view,B: Axial view C: Sagittal view</p>	41
<p>Figure 3.8 Non-manifold Assembly For Mesh Generation</p>	42
<p>Figure 3.9 Scheme of Stages of Avascular Femoral Necrosis adapted for Project</p>	43
<p>Figure 3.10 (A) Stages of AVN: Stage I, Views; A:Coronal view,B: Axial view,C: Sagittal view, Colour Scheme: Pink: Pelvis, Red:Cortical , Bone, Green: Cancellous Bone</p>	44-45
<p>(B) Stages of AVN: Stage II, Views; A:Coronal view,B:Axial view,C: Sagittal view, Colour Scheme: Pink: Pelvis, Red:Cortical Bone, Green: Cancellous Bone</p>	
<p>(C) Stages of AVN: Stage III, Views; A:Coronal view,B: Axialview,C: Sagittal view, Colour Scheme: Pink: Pelvis, Red:Cortical Bone, Green: Cancellous Bone</p>	
<p>(D) Stages of AVN: Stage IV, Views; A:Coronal view,B: Axial view,C: Sagittal view, Colour Scheme: Pink: Pelvis, Red:Cortical Bone, Green: Cancellous Bone</p>	
<p>Figure 3.11 Boundary Conditions</p>	47
<p>Figure 4.1 2D Presentation of Dataset,Views: A:Coronal view,B: Axial view,C: Sagittal view</p>	51
<p>Figure 4.2 Image Processing Results, A. Whole Body Scan, B. Segmented ROI, C. Femur attached with Plevis</p>	52
<p>Figure 4.3 Image Processing Results, Split Mask Function, A.Femur in pink mask & Plevis in Purple, B.Femur, C. Pelvis</p>	53

Figure 4.4 Cortical and Cancellous Bone in 3D, A. Cortical Bone, B.Cancellous Bone, C. Outer Cortical and inner Cancellous Bone	53
Figure 4.5 3-Matic Results, A.Non-manifold Assembly, B. Non-manifold Assembly in high transparency showing intyernal mask	55
Figure 4.6 Four Healthy Models withincreasing mesh densities from Model A-D	55
Figure 4.7 Stages of AVN 3D, Black colour prresents diseased area, A.Stage I, B. Stage II, C. Stage III, D.Stage IV	56
Figure 4.8 Convergence Analysis for Deformation	58
Figure 4.9 Misses Stress Analysis with Increasing Mesh Density	59
Figure 4.10 Plots of Deformation in Healthy Models from Model A-D	61
Figure 4.11 Plots of Misses Stress of Healthy Models from Model A-D	61
Figure 4.12 Deformation w.r.t Stages of AVN	62
Figure 4.13 Mises Stress w.r.t stages of AVN	63
Figure 4.14 Plots of Deformation w.r.t stages of AVN A. Stage I, B. Stage II, C. Stage III, D. Stage IV	65
Figure 4.15 Misses Stress Distribution w.r.t Stage of AVN A. Stage I, B. Stage II, C. Stage III, D. Stage	66
Figure 4.16 Stress at Articulation Points on Pelvis	67
Figure 4.17 Displacement w.r.t Increasing Body Weight in AVN Models	69
Figure 4.18 Mises stress w.r.t Increasing Body Weight in AVN Models	69

List of Tables

Table 2.1	Risk Factors of AVN	15
Table 2.2	Ficat and Arlet Classification of AVN Stages	23
Table 2.3	Pennsylvania Grading System By Steinberg	24
Table 2.4	ARCO Grading System	24
Table 2.5	JOP Grading System	25
Table 3.1	Image Specifications	35
Table 3.2	Material Properties Utilized for Analysis	48
Table 3.3	Mesh Densities For Convergence analysis	49
Table 4.1	Stages of AVN Models with Mesh Densities	56
Table 4.2	Mesh Densities vs Displacement for Converged analysis	57
Table 4.3	Force Calculation w.r.t Body Weight	68
Table 4.4	Validation of Results From Literature	70
Table 4.5	Comparison of Results of Healthy and AVN Models	71

Abstract

The purpose of this study is to conduct computational modeling and simulation of Avascular Femoral Necrosis (AVN) using linear elastic finite element analysis to predict failure in femoral neck. AVN is complex disease of the femoral head. Since femur is the only weight bearing bone in the body, AVN may cause hindered movements and stiffness in the hip joint. Clinical and anatomical significance of AVN has been well established already in the literature. Moreover, it is extensively studied that bone become weaker to provide mechanical support after necrosis. Until now, different animal models have been developed to study mechanical strength and properties of healthy and necrotic bones. However not a single human model is reported in the literature to predict rate of degradation for estimation analysis.

In this research, an effort is made to create computer models using physics of different stages of AVN deploying techniques like image based modeling and Finite Elements. This will enable us to understand more about distribution of stresses localized in the groin area and femoral head w.r.t load alignment.

A mechanically elastic finite element analysis was performed. Our results show that with the progress in bone damage during necrosis, bone behavior changes. Stress become higher in the femoral neck at the point of articulation and shaft become weaker hence prone to fracture. With the increase in the load, femoral neck narrowing risk also increases due to more stresses in this localized region. Von Mises Stress on the superior and inferior regions of femoral neck intersected with frontal plane. Additionally, this study also conducted a mechno-elastic finite element analysis with varying body weights. Increasing weights tend to increase the unborn stresses. Convergence analysis was also carried out for finer meshes. Maximum stress of (146MPa) and displacement of (0.04mm) was observed in stage IV of the AVN models whole bone model whereas in the necrotic region a localized Von Mises stress value of 4.6MPa is observed compared to the health model which was only 1.6MPa. The stresses inferred from this research reasonably correlates with values reported in the literature. We believe that results obtained from this study will be very useful for clinical

prognosis in future; since these computer models will be used as an aid to understand in depth analysis and etiology of necrosis in various stages with numerical accuracy.

Keywords: Finite element analysis, validation, simulation and AVN.

Chapter 1**Introduction****Overview**

This chapter covers the motivation behind this research (section 1.2) and states the research question (section 1.3). It then discusses objectives and contribution of this research (section 1.4). In the last organization of the thesis is explained.

1.1 Motivation

The motivation of this study comes from the fact that orthopedic problems which are occurring worldwide and affecting large number of population and estimated to be increased by 12.91 million by 2050 thus imposing a major burden on the economy. Countries like Pakistan where basic diagnostic facilities are not available situation is much worse. So the author wants to work on a special and uncommon orthopedic condition which sometimes goes undetected. Furthermore, during the under graduate studies, author worked on a research project which was related to determination of vitamin D levels in healthy adults. Later on, when the author came across biomechanics course at graduate level, author opted for a research project which created a link between both the courses.

Bone is a complex material which provides protection and support to the body. It is a reservoir of minerals such as calcium and phosphorus and also provides protection to major organs such as skull protects the brain, rib cage provides protection to the lungs and heart. Bone also work together with muscles and tendon and helps in the movement and locomotion. The femur is the longest and strongest bone in the human body. It bears most of the body weight and provides stability to the core. Bone can lose its functional support and function in the event of damage, this damage can be cause of disease or trauma. There are a variety of diseases associated with the bone such as osteoarthritis, osteoporosis, bone fracture, osteomalacia, avascular femoral necrosis and many more. Avascular Femoral necrosis (AVN) is a rare disease with unclear pathogenesis in which head of the femur is affected due to the loss of blood supply. The head of the femur bone may be lost and also lead to the destruction of hip joint.

The idea of this project originated from the fact that while femur bone is the strongest weight bearing bone in the body, therefore it is important to calculate forces and strain progression during normal functioning as for example, walking, gait, jumping and hopping.

In literature Finite element-based AVN models are generated to predict the biomechanical and pathophysiological features of the necrotic femur head. However, the possibility of weakened femur shaft due to AVN and its ability to support hip structure and overall body weight is not reported objectively. Since, femur bone forms a ball and socket joint with the pelvis, it is important to calculate the degree of disease progression and its effect on the pelvis with respect to the normal body physiology.

1.2 Research Question

“To predict bone strength during different stages of Avascular Femoral Necrosis using mechanically elastic finite element analysis (Linear Analysis)”

1.3 Research Objectives

In order to address the research question as cited, the research is divided into following objectives:

1. To develop computer models of AVN in order to assist clinicians/ doctors for medical prognosis.
2. To create Finite Element models of AVN femoras for insightful study.
3. To understand physics of AVN corresponding real bone damage
4. To predict damage progression in femur neck to create more awareness for support mechanisms in the event of different stages of osteonecrosis.

1.4 Research Contribution

This research directly contributes to the Orthopedic Engineering discipline specific to the AVN studies, which is a deadly disease and also known as the “Coronary disease of hip”. It affect a large number of population, mostly who are in the prime youth and affecting their ability to perform daily activities. Developing image based FE-models of AVN will

help in a reasonable prognosis. As this is first kind of study in Pakistan to develop computer models for AVN , it will serve as benchmark for other researchers and open new dimension for research in this domain.

1.5 Thesis Layout

This thesis consists of 5 chapters in total. A brief description of each chapter is given below.

Chapter 1--Introduction

This chapter provides insight to the topic and states the research question. The objective and motivation behind this research .

Chapter 2--Literature Review

This chapter provides the necessary information about Avascular Femoral Necrosis and past research done in this area of bone biomechanics. A brief review of FEM on AVN is also provided.

Chapter 3--Methodology

In this chapter the methodology opted for this research project is explained. It also gives detailed insight to the approaches used for the creating the models and tools to analyze them.

Chapter 4--Results

In this chapter, all the acquired results are present and discussed. It also gives brief insight of the results how they are obtained and what is their significance. It further critically analyzes the results and validate the simulated values with the numerical values.

Chapter 5--Discussion

In this chapter, results are critically discussed. It also explains the correlation between the past and this present study. Correlation between the healthy and diseased models along with the stage of diseases is explained.

Chapter 6--Conclusion and Future Work

In this chapter a careful conclusion of the study is presented. It also talks about the limitation and problems faced during this study. Recommendation for the future work are also given.

Chapter 2

Literature Review

Overview

This chapter is divided into three sections. In the first section we discuss about the basic science, what is bone and anatomy of hip and femur bone. The second section deals with avascular necrosis (AVN), it's pathogenesis, prevalence, classification and treatment options available. The last section talks about finite element analysis of AVN and different models available to study AVN.

2.1 Basic Science:

2.1.1 What is Bone?

According to Merriam-Webster dictionary(2013) formal definition of bone is “the hard largely calcareous connective tissue of which the adult skeleton of most vertebrates is chiefly composed”. This formal definition does not explain all the functions of bone which are; support and protection to vital organs such as heart and brain. Bone serves as attachment site for muscles, facilitate in movements and also serves as reservoir for ions such as calcium, phosphorus and other trace elements(Shahi Avadi, 2016).

Bones are categorized according to their shape such as flat, long, short or irregular. The flat bones are associated with protection such as sternum, whereas long bones are weight bearing bone such as femur and tibia. The short bones are ones which are associated with support, stability and have limited range of motion(Marangalou, 2013).

Bone has many important functions yet the most important function is mechanical one. For mechanical purposes bone is highly optimized and acts as an excellent biomaterial. It is a strong yet light weight material which has ability to adapt mechanical environment and can repair itself in the event of damage(Marangalou, 2013).

As a material, bone is considered as a composite material with varying degree of porosity and has complex structure (Rho et al., 1998, Weiner and Wagner, 1998). It comprises of organic and inorganic components. The organic components include collagen, peptidoglycans, cytokines and growth factors, whereas inorganic components include calcium hydroxyapatite, calcium phosphate and non-collagenous proteins (Currey, 2002). Bone composition remains constant extracellular but porosity can be varied and changed according to loading conditions.

Bone is a dynamic tissue and is of great physiological importance (Byrne et al., 2010). To understand mechanical properties of bone it is important to understand its hierarchical organization which ranges from macro-scale to nano-scale Figure 2.1 (Beniash, 2011).

A. Macro-Scale

Bone in macrostructure consists of two types of bones called the cancellous bone and cortical bone.

- I. **Cortical bone** also known as *compact bone* and is highly dense
- II. **Cancellous bone** also known as *spongy* or *trabecular bone*.

Cortical bone is mostly present at diaphysis region (shaft) of long bones whereas cancellous bone mostly fills the entire volume and mostly present in epiphysis region of the long bones.

At microstructure level cortical bone and cancellous bone can be distinguished by difference in density and porosity. Cortical bone is less porous whereas cancellous bone has interwoven structure with large cavities and is metabolic active site. It also has ability to repair itself quickly than cortical bone in the event of damage (Reznikov et al., 2014, Rho et al., 1998). Both types of bones are structurally composed of regular, cylindrically shaped lamellae. The difference lays in the orientation of fibril lamellae; in compact bone lamellae are unidirectional whereas in spongy bone lamellae are multidirectional.

B. Micro-Scale

At this level, bone consists of mineralized collagen fibrils which are arranged in sheets called lamellae (Rho et al., 1998). The thickness of lamellae ranges from 3-7 microns and are arranged in concentric layers to form a structure known as osteons. Osteons are categorized as primary osteons and secondary osteons. The secondary osteons or Haversian canal, cylindrical structures with 100-200 microns in diameter are product of primary osteons and have role in bone remodeling (Reznikov et al., 2014).

C. Nano-structure

At nano level main building blocks of bone is collagen fibril. Type I collagen fibrils are most abundant type of protein present in body and play an important role in mechanical properties of bone. The mineral concentration in bone varies from 4 to 7% most important type of mineral present in bone is the hydroxyapatite, $(Ca_{10}(PO_4)_6OH_2)$ a calcium phosphate (Rho et al., 1998, Reznikov et al., 2014) .

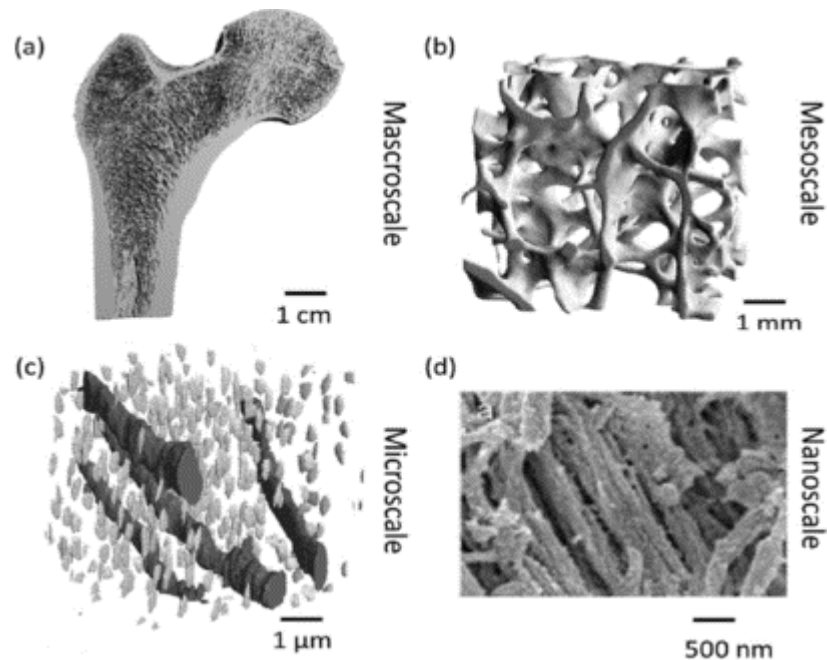


Figure 2.1 Hierarchical Organization of Bone , (a) **Macroscale:** micro-computed (micro-CT) scan of bone showing internal trabeculae and cortical shell ,(b) **Mesoscale:** three dimensional microarchitecture of trabeculae bone of femoral head, (c) **Microscale:** main ultrastructure of the cortical bone (canal network and osteocyte lacunae), (d)**Nanoscale:** scanning electron micrographs of mineralized collagen and fibrils adapted from (Ruffoni and van Lenthe, 2017, Beniash, 2011)

2.1.2 Anatomy of Hip Joint

The hip joint is the ball and socket joint and is most important joint as it serves as a primary connection between the upper limbs and lower portion of the body (Figure 2.2). It consists of spherical femur head and acetabulum along with ligaments and muscles. The muscles and ligaments form a smooth surface and stable joint, which gives a wide range of motion to hip joint and prevent it from dislocation.

Hip joint is synovial type of joint, which are most common type of joints and are characterized by a joint cavity in which bones articulate with one another. At synovial joints, the articulating surfaces are connected by connective tissue or cartilage which allows free movement of bones. These joints are surrounded by ligamentous capsule and have a

synovial membrane. The synovial membrane produces synovial fluid, which lubricates bones and reduces friction between them (Byrne et al., 2010).

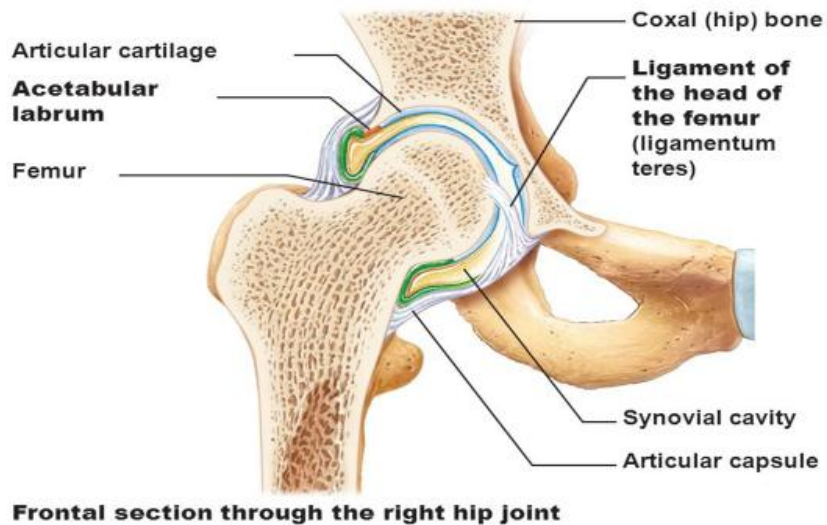


Figure 2.2 Anatomy of the Hip Joint adapted from (Head and Barr, 2013)

2.1.3 Anatomy of Femur Bone

Human femur (Figure 2.3) is the largest, strongest and weight bearing bone also known as “thigh bone”. Femur bone consists of diaphysis (shaft) and two epiphyses (proximal and distal epiphyses). The proximal epiphysis consists of head and neck where the head forms ball and socket joint with hip and neck serves as attachment site for head and shaft of femur bone. Proximally femur has two trochanter areas i.e greater trochanter area and lesser trochanter area. These trochanter areas serve as site of attachment for muscles. The body of femur is known as diaphysis or shaft which is hollow cylindrical structure, the distal part of femur consists of medial and lateral condyles which connect femur bone with knee joint (Gray, 1878).

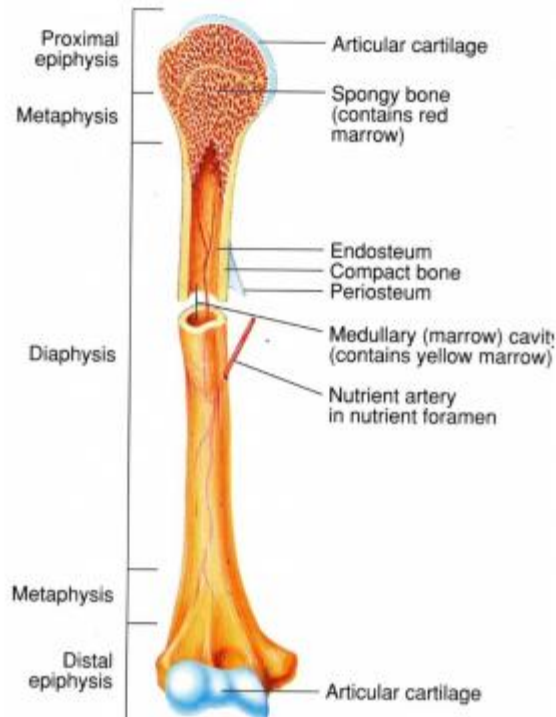


Figure 2.3 Anatomy of the Femur bone adapted by (Marieb and Smith, 2003)

2.2 Avascular Femoral Necrosis

Avascular femoral necrosis (AVN) is an orthopedic condition which is represented by the loss of osteocytes (bone forming cells) due to interruption of blood supply (Saini and Saifuddin, 2004, Malizos et al., 2007, Cooper et al., 2010). The cell death which is caused by the loss of blood supply is known as ischemia. The first case of AVN was studied by Munro in 1738, then after 200 years *Mankin* studied 27 cases and hence coin the term AVN. In literature osteonecrosis is represented by different synonyms such as avascular necrosis (AVN), ischemic necrosis (IN) and aseptic necrosis (Assouline-Dayyan et al., 2002, Jones Jr and Peltier, 2001). All of these terms represent bone cell death and end-stage disease.

In clinical literature, two terms “avascular necrosis” and “osteonecrosis” are often use interchangeably. Both of these terms define bone cell death and end-stage of disease. According to James Andreson in the early stages of disease when bone maintains its structure and only ischemic lesions is present term “avascular necrosis” is often employed to explain such clinical conditions whereas term “osteonecrosis” covers the whole bone pathology ;when bone is damaged enough and has been converted into cartilaginous cyst.

Although these distinctions are not widely supported by clinical literature and therefore border terms are often employed to explain osteonecrosis (Anderson, 2015).

Osteonecrosis can occur at multiple sites such as shoulder, knee and ankle (BARRACK, 1999, Lv et al., 2009, Assouline-Dayana, 2002). In this thesis our main focus is on avascular necrosis of femur head (AVN) which is a destructive disease and mainly affects younger population, who are mostly in third, fourth and fifth decade of life (Mont et al., 1996, Aarvold et al., 2013, Mont and Hungerford, 1995, Shen et al., 2016) as compared to other bone diseases such as “osteoporosis and osteoarthritis.

2.2.1 Occurrence of AVN

Avascular femoral necrosis is mostly prevalent in Asian population as compared to Caucasian population as major load of the disease is reported from the Asian population and is most common diagnosis for patients who undergo hip replacement therapy. According to a study in China by Chiu et al. (1997) reported that in their center 33 patients were undergone through total hip arthroplasty (Chiu et al., 1997). All of them were below 40 years of age and 40% of them were diagnosed with AVN (Chiu et al., 1997). In the same follow up study after 10 years most common diagnosis is avascular femoral necrosis (Chiu et al., 2005). In another study by Lai et al. (2008) on Taiwanese population during period 1996-2004 period, reported that out of 38,323 patients who undergone total hip replacement, 47% were diagnosed with AVN. The average mean age of the patients who were diagnosed with AVN is 50 years and 73% of patients were below 60 years. This study also reported that 79% of AVN patients are male (Lai et al., 2008).

In 2005 a study in Japan showed that 11,400 patients received treatment for the idiopathic osteonecrosis. Most of the patients are in their 40s, 20% males and 18% females are in this range (Fukushima et al., 2010). In Korea, the incidences of femoral necrosis are increasing over time. In 2002 incidences are increased from 20.53 occurrences per 100,00 whereas in 2006 the occurrences increases from 37.96 occurrences per 100,00. These cases account for the between 50% to 60% of primary hip replacement over five years (Kang et al., 2009).

In Taiwan, annually 4000 THR procedures are performed and leading cause of this is AVN. A study by Ching et al. is conducted to find possible etiologies of AVN; they reviewed

medical data from January 2000 to May 2010 with key word “Osteonecrosis” and concluded that 59.1% individuals were diagnosed for AVN with average age of 44.5 to 50.2 years. The prevalence of AVN is more in male (69.3%) as compared to females (49.2%) but risk factors for male and female were found to be different(Tsai et al., 2016).

The rate of incidence of avascular necrosis in European countries are different from Asian countries. A report for England and Wales in 2011 for National Joint Registry stated that 2% of patients were suffering from AVN under gone for hip replacements. This report does not state that percentage of patients who develop secondary osteoarthritis after progression of AVN (Labek et al., 2011). Similar statistics were reported in the Swedish population by Garellick et al. According to their report; between 1995 to 2010, 6,476 cases were reported of AVN and average age of patient is 67.5 years. They also find out that 32% patients develop secondary osteoarthritis following AVN(Garellick et al., 2009). In 2014 another report by National Joint Registry (NJR) for England, Wales and Northern Ireland reported that 22% patients are suffering from AVN are under the age of 30 and have undergone through the hip replacement procedure (Sabah et al., 2015). In a review study for “General Practice Research Database” (GPRD) and The Health Improvement Network (THIN) of United Kingdom by Copper et al. reported cases of AVN between year 1989 to 2003 and also find out that individuals which are under 60 are more prone to AVN(Cooper et al., 2010).

The Australian Joint Registry in 2014 reported that total 3.4% total hip replacement and 1.7% hip resurfacing replacements were performed following incidences of AVN. These demographs doesn't identify the number of secondary osteoarthritis following the AVN.

In United States, actual number of patients are not reported till so far but it is estimated that 20,000 to 30,000 individuals are annually diagnosed for AVN (Orban et al., 2009, Amanatullah et al., 2011, Moya-Angeler et al., 2015). Annually 5-18% of hip arthroplasty are done following progression of AVN (Amanatullah et al., 2011, Kaushik et al., 2012).

2.2.2 Etiology of AVN

There are lot of theories presented to decipher the mechanism of AVN, but its pathogenesis is still unclear. A series of hypotheses are present in literature such as decrease in blood

flow, osteocytes apoptosis, gene polymorphism, genetic causes, immune factors, lipid metabolism and biomechanical factors (Ma et al., 2017). Although AVN is a multifactorial disease with unclear pathogenesis with lot of known risk factors (Lieberman, 2004). Some of the risk factors are listed in the Table 2.1.

Most of the researcher believes that AVN occurs due to loss of blood supply to bone (Assouline-Dayana, 2002). Once blood supply is disrupted, cell death occurs due to loss of nutrients and oxygen. Other factors reported for cell death are genetic predisposition, metabolic factors and factors affecting blood supply such as increased osseous pressure, vascular disruption and mechanical stress (Moya-Angeler et al., 2015).

According to Gautier et al. 2000, AVN of femoral head occur due to loss of vascular supply (Gautier et al., 2000). This loss of blood supply can happen due to variety of reasons which can be (Chen, 2011)

I. Traumatic

II. Non-Traumatic

III. Idiopathic

I. Traumatic AVN

Femur head has intravascular and extravascular supply and an insult to blood supply results into traumatic AVN (Kaushik et al., 2012). Once blood supply is compromised, cell death occurs due to loss of nutrients and oxygen supply (Kaushik et al., 2012). There are many traumatic events such as hip dislocation and bone fracture that results into Traumatic AVN. There are different studies reported in literature which show that after certain period of trauma bone leads toward AVN. One study shows that after the 8 hours of trauma and lack of blood supply bone would lead towards avascular necrosis (Hougaard and Thomsen, 1986). A study on 100 hip dislocations shows that after 6 hour of hip dislocation if not treated there is 53% chances of AVN development (Hougaard and Thomsen, 1986).

Another traumatic factor that leads toward AVN is the fracture of femur head. Fracture causes disruption of vascular supply to the head and ultimately AVN occur if not treated in time (Smith, 1959, Holmberg and Dalen, 1987, Bachiller et al., 2002, Ehlinger et al.,

2011). A brief review on fracture shows that 6-26% fractures of femur lead progress towards AVN (Asnis and Wanek-Sgaglione, 1994, Lu-Yao et al., 2005, Loizou and Parker, 2009).

II. Non-traumatic AVN

Most common causes for non-traumatic cases of AVN are alcohol abuse, corticosteroid therapy, fat emboli and other disease complications such as renal failure, protein C/protein S deficiency. Among these risk factors, alcohol and corticosteroid are the most important causes of AVN and ranked higher for the development of AVN.

Alcohol abuse is reported to be leading cause of AVN 10% to 74% whereas corticosteroid use is ranked second higher cause 5-58%. The possible mechanism of alcohol is that it causes mesenchymal cells not to differentiate in bone forming cells. The corticosteroid use, ranked second major cause of non-traumatic cases of AVN. The incidences of steroid use ranges from 5-58%.

Human immunodeficiency syndrome (HIV) is also associated with the AVN and is presented after diagnosis of HIV, however mechanism of disease is not clear. It is believed that highly active anti-retroviral therapy (HAART) was the biggest risk factor.

Allogenic bone transplantation is considered another important risk factor. In USA, 10% of patients who receive allogenic bone transplants developed AVN within 1-2 months after treatment.

III. Idiopathic AVN

When bone is damaging asymptotically (without any apparent reason) than the condition is known as Idiopathic avascular necrosis and is diagnosed when the only choice of treatment available is hip replacement therapy. In literature a lot of idiopathic cases are reported and the leading cause of such cases is considered to be genetic one (Chen, 2011). A study conducted on Japanese family by Miyamoto et al. reported a mutation in type II collagen protein which is responsible for the osteonecrosis in children (Miyamoto et al., 2007). A study on Taiwan population reported a gene responsible for hereditary osteonecrosis (Liu et

al., 2005). Glueck et al and Jones et al reported hereditary conditions in the Western countries.

Traumatic	
Femoral neck fracture	Vessel disruption
Hip dislocation	Extensive burns
Non-traumatic	
Alcoholism	Smoking
Steroid	Radiation
Contraceptive use	Pregnancy
Diseases	
Sickle cell anemia	Diabetes mellitus
Hyperparathyroidism	Cushing disease
Gout	Collagen diseases
Pancreatis	Resistance to activated protein C
Hemoglobinopathies	Chron's disease
Erythematosus	Hemophilia

Table 2.1 Risk Factors of AVN adapted from (Malizos et al., 2007, Séguin et al., 2008)

2.2.3 Stages of AVN

To understand AVN it is very important to understand different stages of this orthopedic condition. Each stage represents a clinical condition which if treated in time will not only limit the disease progression but ultimately also save joint. As true etiology of AVN is still unclear and there is not true link is present between the etiology and pathogenesis of disease. It is also believed that there is no link between stage and disease progression, that

is some time patient with advance stage of disease are asymptomatic as compared to other patients with early stage which are symptomatic.

Figure 2.4 explains events that leads toward AVN. There are lot of factors which trigger onset of AVN, pathway may vary but disease progression remains same in majority of the case.

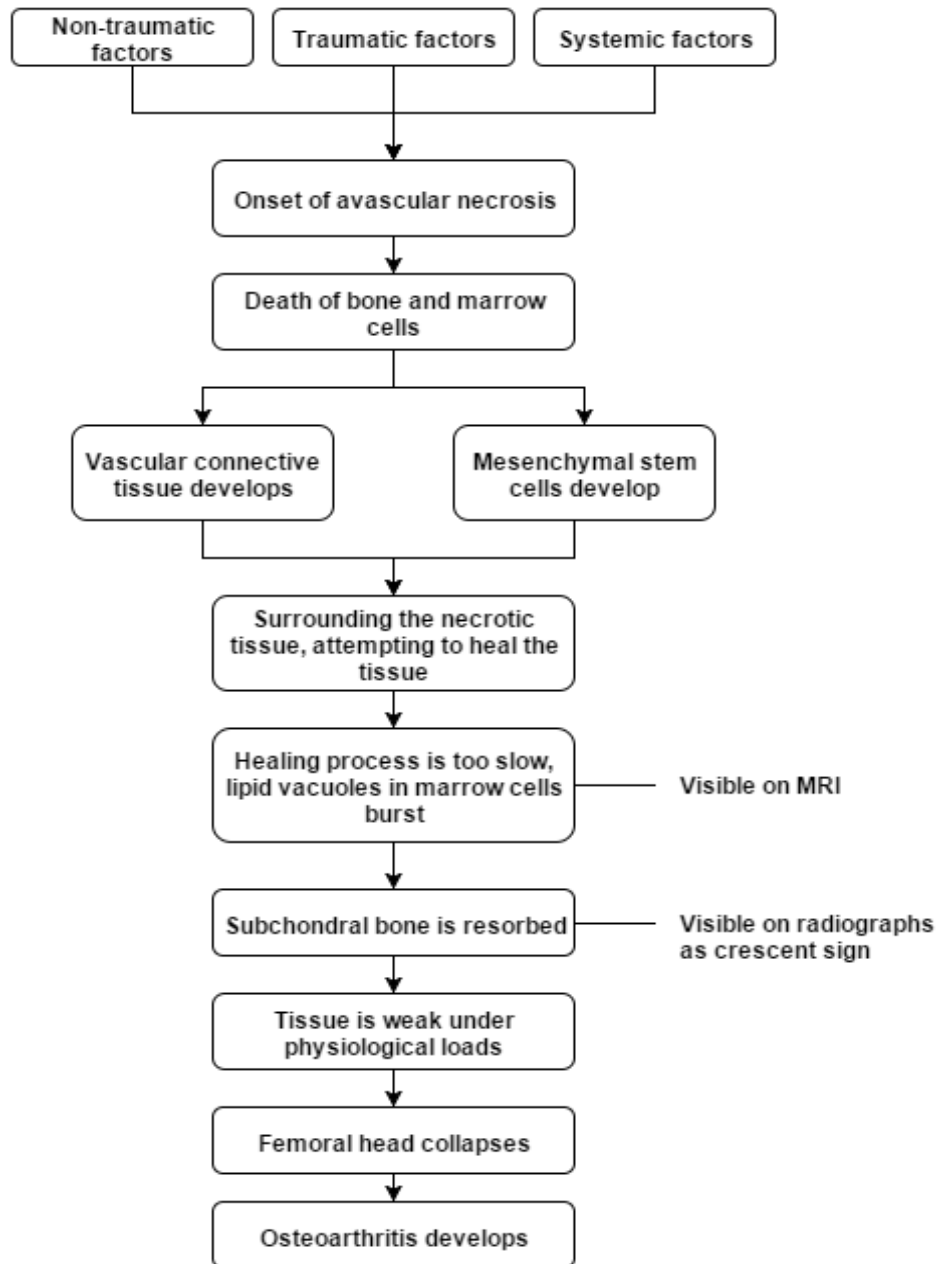


Figure 2.4 Series of events for the onset of AVN Adapted from(Shahi Avadi, 2016)

Bone necrosis starts when it is deprived of blood supply. The interruption of blood supply can occur because of various risk factors which are explained above in table 2.1. Once bone is blood deprived it starts degrading and condition is further alienated if not treated properly and ultimately develop necrosis. There are three type of zones present in the necrotic femur; avascular zone, reparative vascular zone and normal vascular zone Figure 2.5. These zones depends upon the number of arteries involved in site of damage.

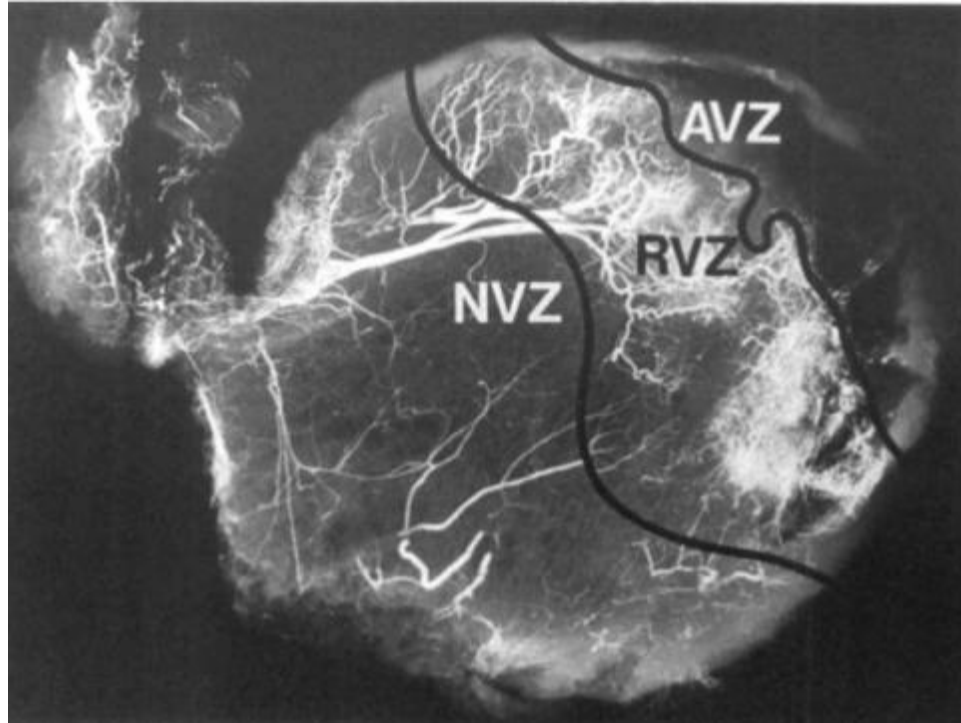


Figure 2.5 Micro-angiographic Study of Femur Head with AVN, adapted from (Shahi Avadi, 2016)

When AVN starts to progress it affect all the cell types present in the bone and bone marrow. The bone marrow generally consist of fat cells known as adipocytes (yellow marrow). These cells have a small nuclei, cytoplasm and have a lipid vacuole. In the event of bone damage these vacuoles are not affected by cell death and they remain unchanged for some time and can be detected by the magnetic resonance imaging (MRI) which otherwise can be distinguished from healthy cells figure2.6(a) figure 2.b).



Figure 2.6(a) Radiograph of early Stage of AVN with no visible change. Adapted from(Anderson, 2015)

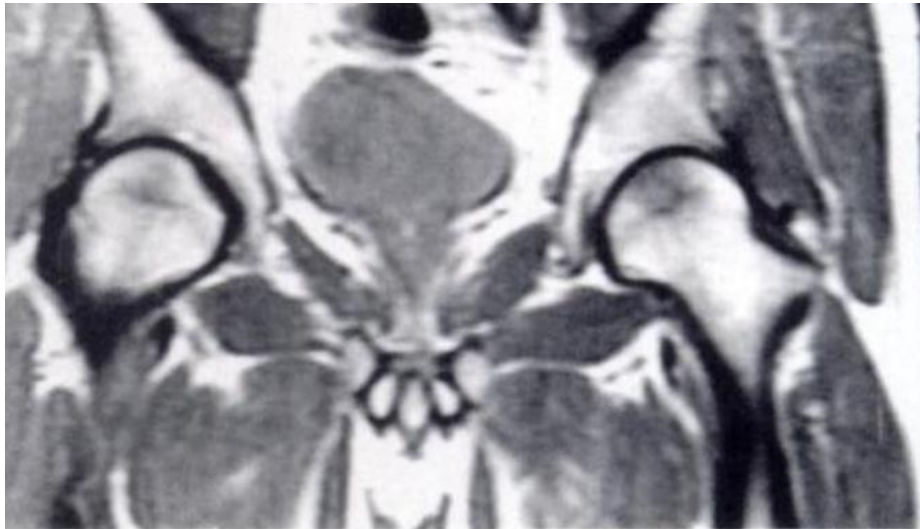


Figure 2.6 (b) MRI of Stage 0 AVN Adapted from(Anderson, 2015)

As disease progress in a few days or weeks mesenchymal stem cells starts to develop at the necrotic region. The osteocytes develop in necrotic area and start healing process, whereas osteoclast start eating dead bone and osteoblast starts bone growth. Although it is believed that the rate of bone degradation is much faster than the bone formation in AVN. Bone tries

to repair itself in the event of damage and forms a band near the necrosis area known as sclerotic band as shown in Figure 2.7. At this phase femur head dose not lose its structure and joint space is also retained(Anderson, 2015). During later stages when sclerotic band forms and adipocytes bursts their contents are spilled and get calcified. At this stages MRI shows clear picture of bone necrosis.

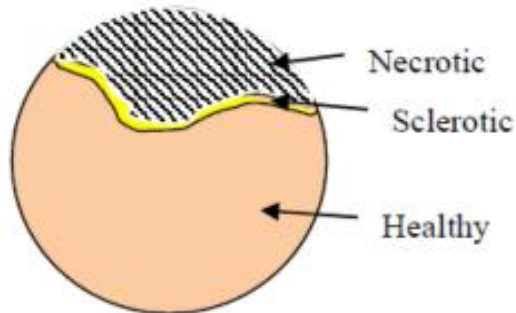


Figure 2.7 Representation of Necrotic and Sclerotic area, adapted from(Anderson, 2015)

Bone has capacity to remodel itself in the event of damage but in case of bone necrosis bone remodeling process is ill adapted. This results in the resorption of subchondral bone and mechanical properties of bone are weakened. When mechanical properties are weaken ,bone cannot bear mechanical stress and other physiological factors. This results in bone fracture which is known as crescent sign figure 2.8. This crescent sign is visible on radiographs as well as other imaging modalities (Saini and Saifuddin, 2004).

The disease progress 1 to 5 years in different individuals. The end stage of disease is collapse of femur head and development of secondary osteoarthritis. At this point patient feels pain and femur head lost most of its structure.

2.2.4 Diagnosis

Diagnosis of AVN is like any other orthopedic condition. It generally starts with the medical and family history, physical exam and further to imaging techniques. If certain medical conditions are linked then a differential diagnosis is done. Mostly patients comes with groin pain.

2.2.5 Diagnostic Techniques

There are different diagnostic techniques available to diagnose AVN such as Radiography, Magnetic Resonance Imaging (MRI), Computed Tomography (CT), DEXA Scan (to calculate bone density).

The choice of the imaging technique employed to diagnosis AVN depends upon stage of the diseases. A variety of imaging techniques are discussed in literature to diagnose AVN and most common imaging modality is radiography, but it has some limitations. Initial stages of AVN are not diagnosed by plain radiography. Plain radiographs show AVN when subchondral bone is fracture and has a characteristics crescent sign Figure 2.8 .

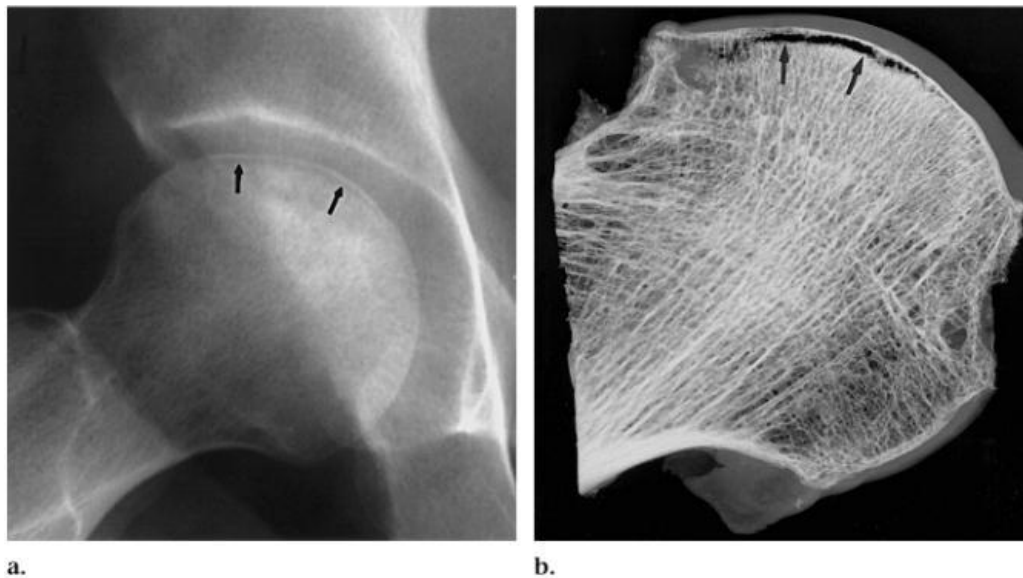


Figure 2.8 (a) Femur head showing the area of hyperlucency with arrows (b) Femur head showing subchondral fracture with crescent sign. Adapted from (Pappas, 2000)

With the advancement in imaging modalities it is possible to diagnose AVN in early stages. Magnetic resonance imaging (MRI) is the most sensitive and accurate method to diagnose AVN in early stages. It can detect signal changes in bone marrow and osteocytes cells death. MRI is important for early diagnosis and quantification of AVN(Saini and Saifuddin, 2004) and has major role in accurate prognosis of AVN as choice of treatment depend upon the diagnosis of AVN(Jergesen et al., 1990).

Other imaging modalities are also used to diagnose AVN such as Computed tomography (CT), but they have accuracy over MRI for the early detection of AVN. In a study capability of MRI, X-ray CT and radio nucleotide sequencing were compared with controlled group and it was found out that MRI is more sensitive diagnostic technique for early diagnosis(Mitchell et al., 1986).

2.2.6 Staging and Classification of AVN

There are several classification systems present to classify AVN. These classification system helps to diagnose, quantify the stage of disease (Assouline-Dayyan et al., 2002). According to literature present to date more than sixteen system are present for staging AVN, but three to four systems are widely in use. These classification systems depend upon the severity of symptoms and radiographic findings. Although there is no consensus on different classification systems therefore it is difficult to analyze and compare data from different sources (Choi et al., 2015).

Of the many systems available for classification of AVN Ficat and Arlet system was the first system developed in late 1960's (Table 2. 2), then University of Pennsylvania grading system also known as Steinberg classification (Table 2.3), the Association Research Circulation Osseous System (ARCO) grading system (Table 2.4) and Japanese Orthopedic Association grading system (Table 2.5).

Ficat and Arlet system of classification is the basic system of classification which starts as 3 stage system then with the advancement in the diagnostic methods, it expands to four and six stages. The University of Pennsylvania and ARCO grading systems are comprehensive one and are extension of basic Ficat and Arlet grading systems. These systems use the information from the radiographs, MRI and Scintigraph.

Of all the systems present for grading these four systems are reported in 85% of the studies. The Ficat and Arlet is reported in 63% of the studies, University of Pennsylvania 20%, ARCO in 12% and Japanese Orthopedic Association system in 5% studies(Choi et al., 2015).

Since there is no mutual agreement present on grading system therefore the prognostic feature depend upon several factors which are size of the lesion, extent of subchondral fracture and location of lesion(Choi et al., 2015).

Size and location of the necrotic lesion are important prognostic feature of AVN but they cannot fully explain whether collapse occur or not. In literature general consensus is present for lesion size that is <15%, 15-30% and >30% are small, medium and large. This lesion size calculation is done by calculating the extent of lesion damage by two angular calculation in the sagittal plane and coronal MRI slices.

Stages	Radiographic findings
1	None (Only evident on MRI)
2	Diffuse sclerosis, cysts (Visible on radiographs)
3	Subchondral fracture (Crescent sign, with, or without head collapse)
4	Femoral head collapse, acetabular involvement, osteoarthritic degeneration

Table 2.2 Ficat and Arlet Classification of AVN Stages Adapted from(Anderson, 2015)

Stage	Radiographic findings	Sub-classification		Involvement
0	Normal or non-diagnostic radiograph, bone scan and MRI	Not applicable		
I	Normal radiograph. Abnormal bone scan and / or MRI	A	Mild	<15% of head involvement as seen on radiograph or MRI
		B	Moderate	15% to 30%
		C	Severe	>30%
II	Abnormal radiograph showing "cystic" and sclerotic changes in the femoral head. Head remains spherical	A	Mild	<15% of head involvement as seen on radiograph or MRI
		B	Moderate	15% to 30%
		C	Severe	>30%
III	Subchondral collapse producing a crescent sign below subchondral layer.	A	Mild	Subchondral collapse (crescent) beneath <15% of the articular surface
		B	Moderate	Crescent beneath 15% to 30%
		C	Severe	Crescent beneath >30%
IV	Flattening of the femoral head	A	Mild	<15% of surface has collapsed and depression is <2mm
		B	Moderate	15% to 30% collapsed or 2-4mm depression
		C	Severe	>30% collapsed or >4mm depression

Table 2.3 Pennsylvania Grading System by Steinberg adapted from (Anderson, 2015)


Stage	0	I	II	III	IV
Findings	All present techniques show normal or non-diagnostic results	X-ray, CT are normal, at least one of the techniques below is positive	No crescent sign, x-ray abnormal: showing sclerosis, osteolysis, local porosis	Crescent sign on x-ray and/or flattening of the articular surface of the femoral head	Osteoarthritis, joint space narrowing, acetabular changes, joint destruction
Techniques	X-ray CT Scintograph MRI	Scintograph MRI Quantitate using MRI	X-ray CT Scintograph MRI Quantitate using MRI	X-ray CT Quantitate on X-ray	X-ray only
Quantitation	No	% Area involvement Minimal A <15% Moderate B 15% to 30% Extensive C >30%		Length of crescent A <15% B 15% to 30% C >30%	No
				% Surface collapse and dome depression A <15%, <2mm B 15% to 30%, 2mm-4mm C >30%, >4mm	
Sub-classification	No				No

Table 2.4 ARCO Grading System Adapted From (Anderson, 2015)

Stage	Finding	Quantitation	Location
1	Demarcation line, subdivided by relationship to weight-bearing area	1A	Medial
		1B	Central
		1C	Lateral
2	Early flattening WITHOUT demarcation line around necrotic area		
3	Cystic lesions, subdivided by site in the femoral head	3A	Medial
		3B	Lateral

Table 2.5 JOA Grading System Adapted from (Anderson, 2015)

2.2.7 Treatment

There are many treatment options available for the AVN. The main goal of the treatment is to provide relief to patient from pain , to preserve joint and provide aid in performing daily normal activities. The choice of treatment depend upon certain factors which are

- a. Age
- b. Physical Condition
- c. Extent of the bone damage
- d. Stage of the disease

There are two types of treatment options available; non-operative and operative. The choice of treatment depends upon the stage of the disease and extent of bone damage

1. Non-Operative Treatment:

The non-operative treatment options are employed when the AVN is in initial phases and bone is not damaged. Some of the treatment option are enlisted as

- Medication : to relief pain
- Limit range of motion
- Support by the crutches or walker to minimize
- Avoid other risk factors such as corticosteroid and alcohol use
- Use of the hyper baric oxygen chamber
- Shock wave therapy

2. Operative Treatment

The operative treatment options are used when extent of damage is beyond repair and only choice of treatment is available. The goal of surgical treatment is to repair and provide support to the joint. Some of the most common treatment options are core decomposition, bone grafting, rotational osteotomy and total hip replacement therapy.

Core decomposition is prophylactic surgery which is usually done before collapse. It is done by drilling hole in the necrotic bone. The main aim of this method is to improve blood circulation and decrease bone pressure. The core decomposition procedure is usually suitable for Ficat I and II stages. Core decomposition along with bone grafts allows bone to start the healing process by forming new bone.

Rotational osteotomy is that; femur head is rotated either anteriorly or posteriorly along longitudinal axis of bone. This twisting of head reduces pressure in the bone and also allowing healthy area to bear stress.

Hip arthroplasty or total hip replacement therapy is done when the joint fully damaged and bone is beyond repair. In this treatment joint is removed surgically and replaced with artificial one. THA has been an important factor in pain relief. This is usually done to preserve joint. THA is mostly done on younger patients so that they can perform daily activities without any difficulty.

2.3 Finite Element Method and AVN

2.3.1 Introduction to FEM:

The mathematical approach to solve any problem from any discipline to get an approximate result is known as the Finite element method. In this method the bigger problem is divided into small problems which are connected by nodes and they mimic the original system/problem (Mustansar, 2015)

The term FEM is coined in 1960's. Since then this is used by engineers to study stress and strain in different areas such as heat flow, load transfer, stress analysis and many others. In the recent decades FEM play a major role in biomechanics.

Over the past 40 years, bone is most common biomaterial use to simulate mechanical behavior by finite element analysis and has substantial impact on bone research. Thus it is very important to plan finite element analysis very carefully as small change in anatomy, boundary conditions and material properties would lead to errors or false results. The choice of element type is very important, different types of elements have different types of assumptions and can lead to different type of results. The most common type of elements are tetrahedral as they are easy to solve and take less computational time. To predict stresses and deformation iterative methods are used. The purpose of iterative method is to simplify the problem and to get analytical solution of the problem. To check whether analytical solution is good enough convergence analysis is done with varying mesh densities. The steps involved in the FEM are explained in the figure 2.9.

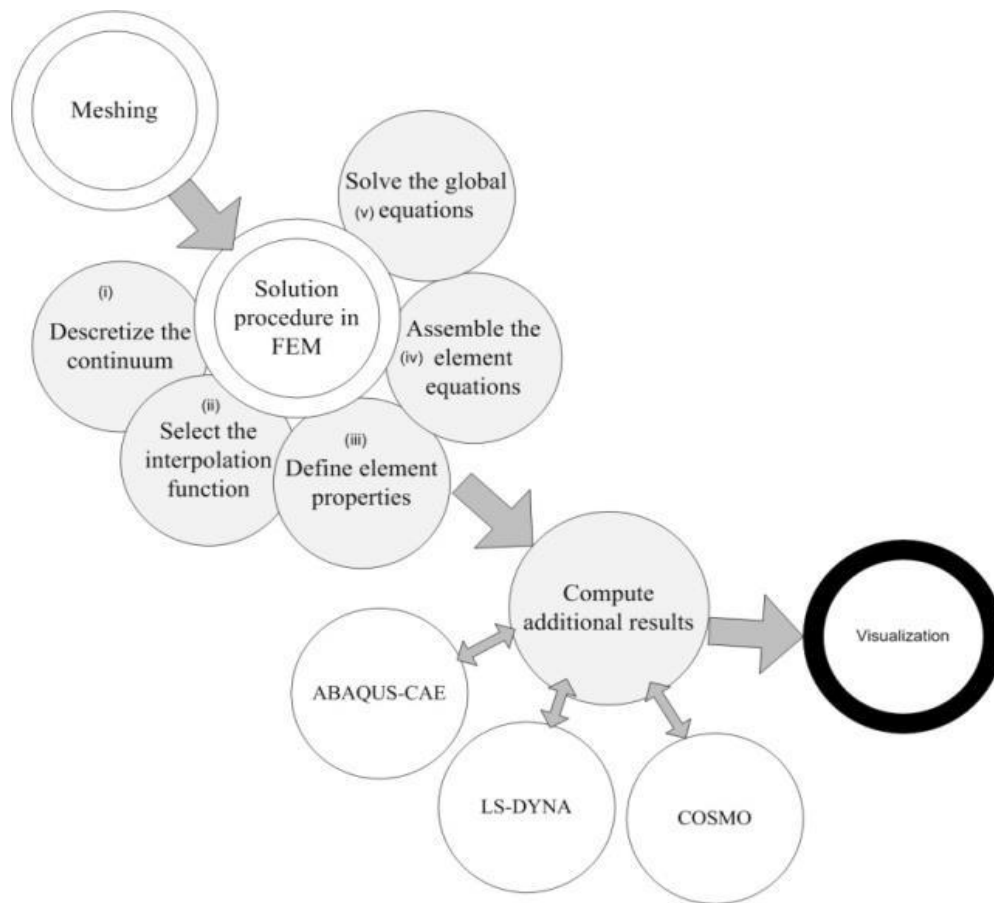


Figure 2.9 Steps of Finite Element Analysis adapted from (Mustansar, 2015)

In 1972 Brekelmans first used FEM to investigate stresses in human bone under physiological conditions. Finite element method has vast applications in orthopedics biomechanics from mechanical behavior of bone in normal and pathophysiological condition, bone remodeling and bone fracture analysis.

Since determination of mechanical stresses is important in human bones under natural physiological conditions for both clinical and research purposes hence FEM is most important in the Orthopedic Mechanics. As it is not possible to measure stress strain non-invasively in living tissues so FEM is the ultimate choice as it measures stress and strain non-invasively. These analysis requires exact geometries of bone which is obtained from CT or MRI data of bone.

2.3.2 FEM and AVN:

Finite element is promising and valid technique in modern literature to answer the scientific questions as well as bringing solutions to clinical research. A lot of studies are conducted on AVN to investigate progression and mechanical strength of femur bone. Brown et al. (1981) was the first one to investigate mechanical properties of human femur AVN. They tested eight post-collapse and one pre-collapse femur head by uniaxial compression testing. In this study three different types of cubes are taken for testing that are completely necrotic, sclerotic region and adjacent to the necrotic region. The results from the study show that there is 51% reduction in the bone strength for the necrotic bone part. The sclerotic region adjacent to the necrotic region does not show any statistically significant reduction in strength. The pre-collapse group also shows similar reduction in strength and stiffness. Thus it is concluded that there is visible change in strength and mechanical properties in femur AVN in early stages.

Later on in 1992 Brown et al. studied mechanical properties of bone using finite element method. The main purpose of the study was to investigate mechanical effect of subchondral plate on the under lying damage bone due to AVN. They found out that the structural integrity of subchondral bone was unaffected and stress levels were 70% more in the bone near to cancellous bone. This study shows that the onset of collapse in AVN is dominated by the structural degradation of cancellous bone rather than the subchondral plate.

Brown et al. in 1993 further studied the effect of core decomposition on AVN. The main purpose of the study was to investigate the mechanical integrity of the necrotic femoral head using linear elastic model. For this study they created lesion in the femur head from MRI data and physically attenuated its modulus by 75% and strength by 50% from their previous study. The results of the study show that it is the loss of the mechanical strength of cancellous bone whose causes high stress in the necrotic bone and is responsible for the fracture in subchondral plate in later stages of AVN.

The study by Brown et al. remains a standard for many other studies. In 2002, Yang et al. conducted a study on femoral head AVN. They cited Brown et al. to assign material properties to necrotic bone. They uses 445MPa and 218MPa, and yield strength of 19.4 and 5.5MPa respectively. They assumed bone to be anisotropic and ignored all the effects of cortical bone. A Poisson ratio of 0.33 was used throughout, neither cartilage nor cortical bone was modelled. MRI scans of 55 patients with AVN were gathered. Location and lesion size were considered to be as a cone. For the determination of stress index which is defined as ratio of the measured stress over yield strength and compare to highest stress index and location of the fracture site in the necrotic head. They studied the static failure and fatigue fracture. In normal healthy bone the stress index was considered to be unity. The static failure stress index was greater than the unity whereas the same stress index was much lower than unity in fatigues fractures. The same stress index was found in the necrotic head when the conical angle of the lesion was less the 110 degree. The authors concluded that the lesion of this size cannot cause fracture because it was compared to the healthy bone.

In 2005 a series of studies are conducted in post collapse AVN to find out the relationship of cartilage degeneration in the femur head of AVN. A series of tension, compression and shear tests are performed on the cartilage and subchondral plate. They found out that the tensile strength of the cartilage is decreased due to the degeneration of the cartilage in AVN, whereas less correlation is present between the shear and compressive strength. These results were compared with the osteoarthritis bone and it was found that the cartilage degeneration in AVN was different histologically and mechanically than from osteoarthritic bone.

There are many complications associated with the osteonecrosis hips and the major one is the development of osteoarthritis. Daniel et al. (2006) simulated the contact stress index in the femur head with the major articulating surface. According to the study the load bearing capacity of the hip is decreased as the necrotic lesion size is increased and is sensitive to the load vector direction (Daniel et al., 2006).

In literature there are many studies present which simulate the AVN femur head according to the lesion size and location of the lesion. In a most recent study by Zhou et al. in which they modelled the physiological (healthy) and pathophysiological (necrotic) model. They use a previous study by Brown et al for the material properties assignment. The outcome of the study was lesion play a major role in the stress distribution in the AVN. Similar study was done by Bae et al. with same material properties. They considered the lesion as simplified structure like cone at an angle 100° . However their study did not measure the effect of lesion on the stress.

Bone is highly anisotropic structure but all the studies on the AVN till to date considered the bone and necrotic lesion as homogenous material and assign the same material properties to both. This may be true given the fact that lack of literature is present on the necrotic lesion and the complexity of femur head structure with lesion. So to cover this aspect multi-scale modelling approach was employed by Vaughan et al. In this approach they model the tissue fibers from micro to macro structures. The concept of this approach is to predict the elastic properties as a function of radiographs.

2.3.3 AVN Models

In literature several attempts have been made to create a valid AVN model to study the natural progression of disease. As it is not possible to study the natural progression of disease in human models therefore till to date several animal models are developed for this purpose. AVN is induced in the animals to study the mechanical and biological aspect of the disease. There are two types of models created non-traumatic models and traumatic models which are explained below in detail.

2.3.3.1 Non-Traumatic Models

Since corticosteroid abuse is one of the major risk factor for the development of AVN, so many authors used this approach for the induction of AVN in the animals. Various animals such as mice, rats, pigs, rabbits and ponies are used to model AVN. Although AVN is induced successfully in these animals but they do not reflect the natural mechanical aspects of the AVN as are seen in humans. This may be of the effect that all these animals are quadrupeds not the bipedal and also the multifactorial nature of AVN.

The other major risk factor in humans for the development of AVMN is alcohol, which have been used to induce AVN in animals. A study by Manggold et al. (2002) develop a model of sheep AVN by the induction of ethanol in the sheep head. The sheep develop the necrotic lesion in the head but the sheep did not lead to the mechanical collapse of femur head after the 12 weeks of alcohol administration.

Some of the other novel methods have been reported in literature for the induction of AVN in femur head of animals. Some of these methods are hormone induction in rabbits, autoimmune activation in rats, intravascular coagulation in rats, rabbits and pigs, induced hypersensitivity in rabbits and inducing oxidative stress and cryogenic freezing in rats (Shahi Avadi, 2016).

2.3.3.2 Traumatic Models

Several traumatic animal models have been created in literature to study femur head AVN. the trauma occurs when disruption occur in the vascular supply to the femur head. In humans the most common cause of the traumatic AVN is the fracture of femur head. There is a study conducted in 1996 by Seiler et al. to show that the if vascular supply is disrupted then the AVN occur. They induce the osteotomy in the head to cause a fracture. After 8 weeks of monitoring they reported that there is decrease in the blood flow to the femur head and histology works confirmed the development of AVN.

Since all the models developed so far are quadruples therefore these models cannot explain the exact mechanism of AVN progression. To overcome this problem Conzemius et al. (1999) developed an emu model to develop a human like mechanical model. The theory

behind this model was that all the previous models were quadruples and they failed to progress the end stage of AVN but Emu is a bipedal animal and is highly active and represents more changing environment therefore it may result in to progress into the end stage of AVN and mechanical failure of the hip due to the AVN. There were 19 emu and AVN was induced by ischemia or cryogenically. Out of 19, 18 emu develop end stage AVN with 6 showing the crescent sign. This study was successful in developing the end stage of AVN just as found in humans but it does not compare the properties of collapse bone with human femur head.

Missing link in the literature

In literature a lot of studies are present on AVN explaining the natural progression of the disease. Animal models are developed to study the AVN but up till now no mechanical models are generated to study the AVN. This represents a gap in the literature, so there is need to develop the mechanical models for the AVN which would help in the better prognosis and treatment of AVN.

CHAPTER 3

Methodology

Overview

This chapter talks about the materials required and methods adapted to create healthy and diseased models of the femur bone. This study is divided into three-fold stages. In first stage, computed tomography scans were used for image based modeling by using Mimic Innovation Suite 19, in second stage FEM was performed for both healthy and diseased models under physiological loading conditions. In last stage, the simulation results were validated by using a mathematical solution (analytical solution).

3.1 Work Flow

To investigate stress and deformation in femur bone mechanically is difficult and expensive process, as physical specimens are required for mechanical testing. To cope with this difficulty computer based models are generated. The methodology adopted for this project is explained in Figure 3.1

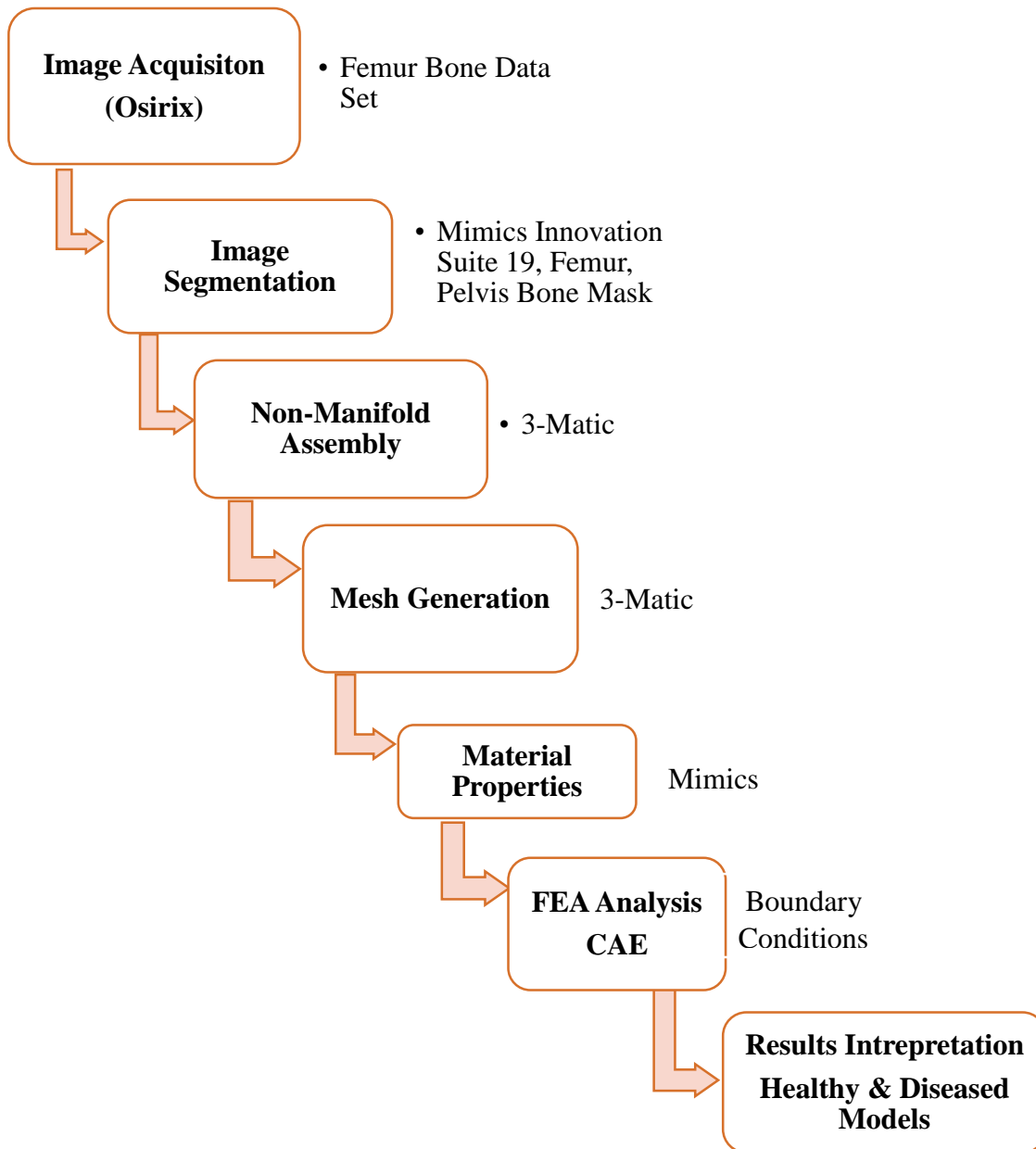


Figure 3.1 Project Flow Diagram

3.2 Image Acquisition:

Computed Tomography scans of femur bone are used in this study with pelvis intact. Images were chosen with reasonable internal structures for both healthy and necrotic models. Dataset was obtained from hospitals first which was missing a lot of information regarding planar images and axial geometry which is why images were not used to create more models. Moreover the quality was too vague. Therefore authors fetch dataset from online DICOM image repository, Osirix (<http://www.osirix-viewer.com/resources/dicom-image-library/>) in November 2016.

The dataset was human femur model with a whole body normal computed tomography angiography (CTA) study of a 43 Years male. Images were acquired on a CT 16 scanner. The femur was 497.07 mm in length with an adult weight of 50 Kg. The image specifications are given the table 3.1

Image Specifications	
Pixel Spacing (2D)	0.7412875\0.7421875 mm
Source to Image Distance	1040 mm
Total no.of slices	1559
Slice Thickness	2 mm
X-Ray Tube Current	354 mA

Table 3.1 Image Specifications

Dataset was later refined, and noise was removed from images using advanced filters.

3.3 Image Segmentation

For segmentation, an advanced image processing suite was utilized known as **Materialize Interactive Medical Image Control System (MIMICS)** developed by Materialize Belgium. This software is an interactive tool which provides ability to visualize and segment CT data for correct image segmentation. For this project a recent version of MIMICS known as *Mimics Innovation Suite 19* was employed. Software consists of two modules, Mimics and 3-Matic. In Mimics image segmentation is done and 3-Matic deals with mesh generation. The process flow diagram of this software is shown in Figure 3.2.

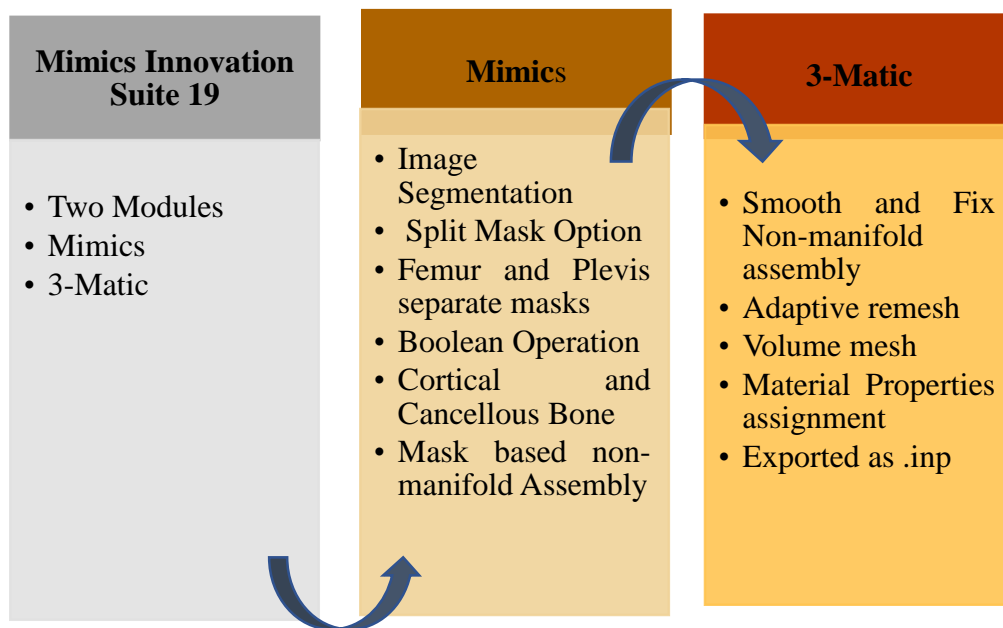


Figure 3.2 Process Flow Diagram of Mimics Innovation Suite 19

The data was thresholded using predefined values for Bone CT data and a whole-body 2D view was calculated as shown in Figure 3.3. As whole-body scan was not required for the present study so region of interest (*ROI*) was cropped out by using *crop mask* feature available in the software, i.e femur attached with the pelvis, Figure 3.4. For simplification purpose and to limit the computational cost, only right femur bone attached with pelvis was used for present study Figure 3.5. Combinations of “mean” and “median” filters were applied to remove any noise and unwanted information. In Mimics Innovation Suite, a special *Split mask* feature is available which splits different anatomical structures into separate masks. Femur has a ball and socket joint with pelvis, so split mask option was

utilized to separate out femur and pelvis in two distinct masks Figure 3.6 (a, b, c). In Figure 3.6 (a) split mask function is presented by two different colors; Pink color presenting femur bone mask and Purple color presenting Pelvis mask. Figure 3.6 (b) presented separated femur bone after split mask application and Figure 3.6 (c) presents pelvis

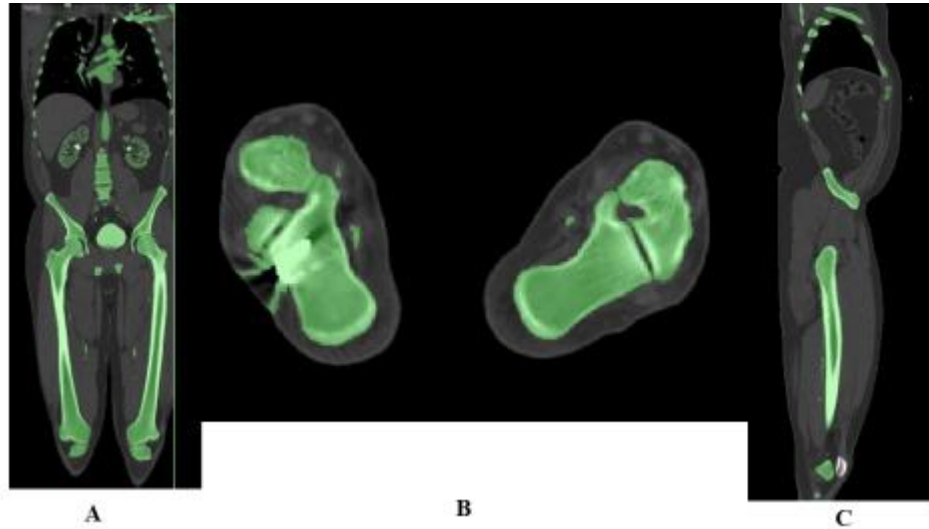


Figure 3.3 Predefined Threshold Values

Views; A. Coronal view, B. Axial view, C. Sagittal view

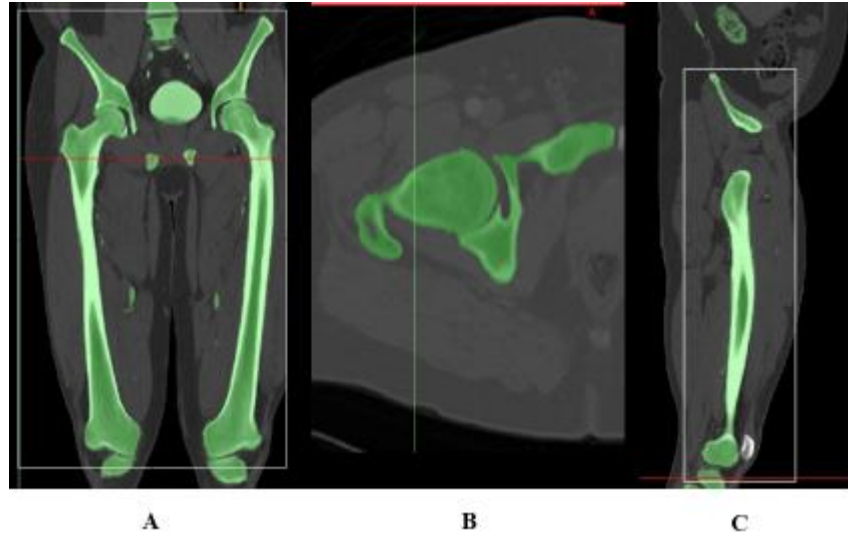


Figure 3.4 Cropped ROI 2DViews; A. Coronal view, B. Axial View, C. Sagittal view

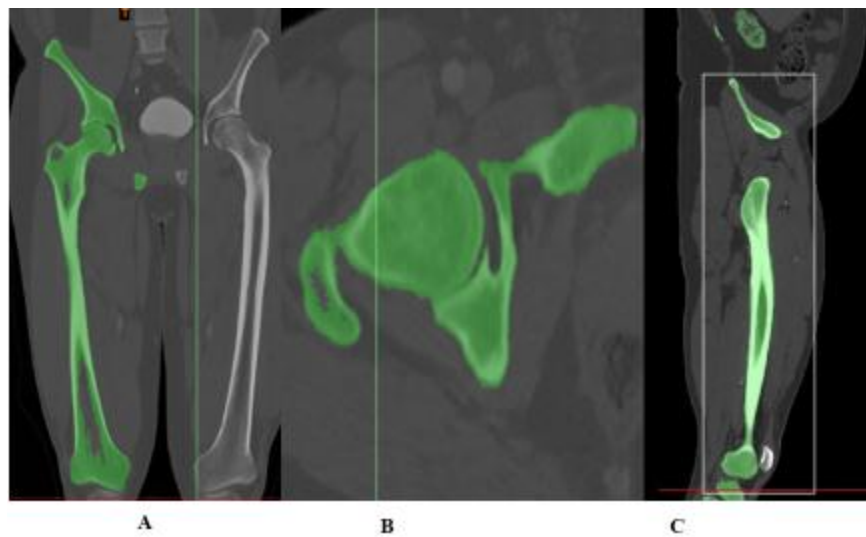


Figure 3.5 Right Femur bone attached with Pelvis Model 2D Views; A. Coronal view, B. Axial view, C. Sagittal view

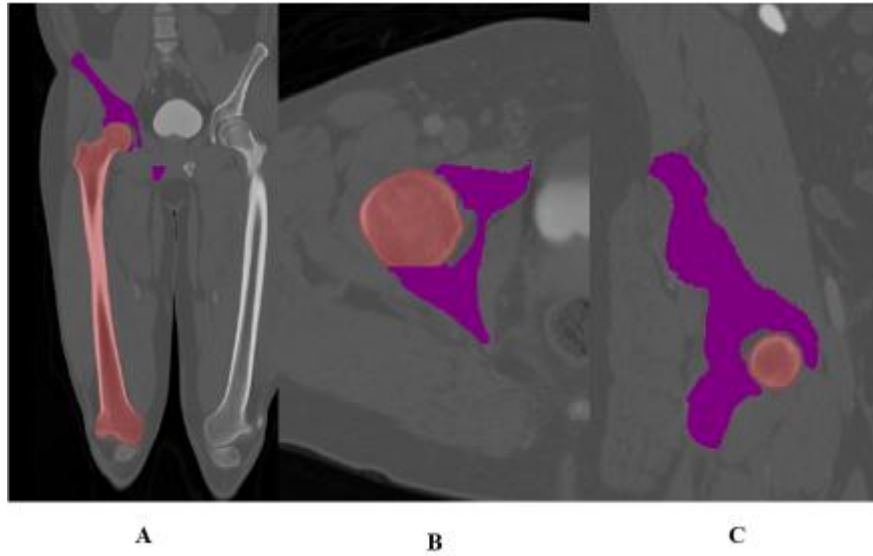


Figure 3.6 (a) Split Mask Function 2D Pink color: Femur bone and Purple color: Pelvis Views; A. Coronal view, B. Axial view, C. Sagittal view

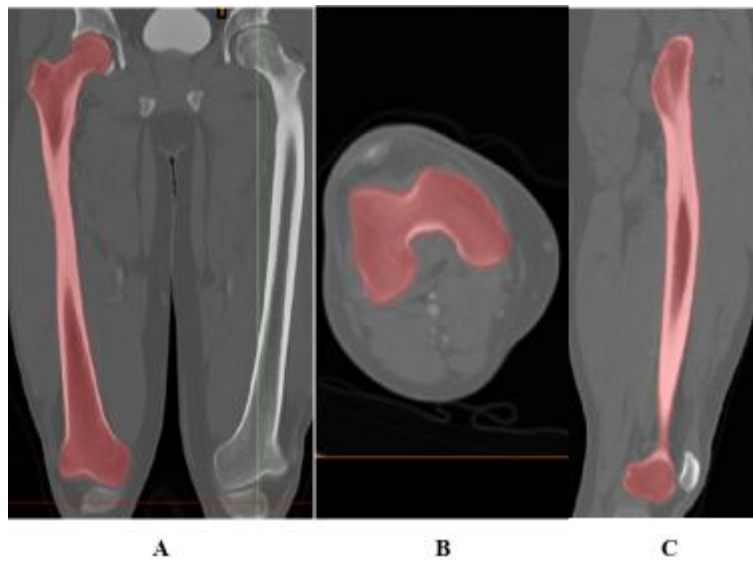


Figure 3.6 (b) Femur Bone after Split Mask Function Views. A. Coronal view, B. Axial view, C. Sagittal view

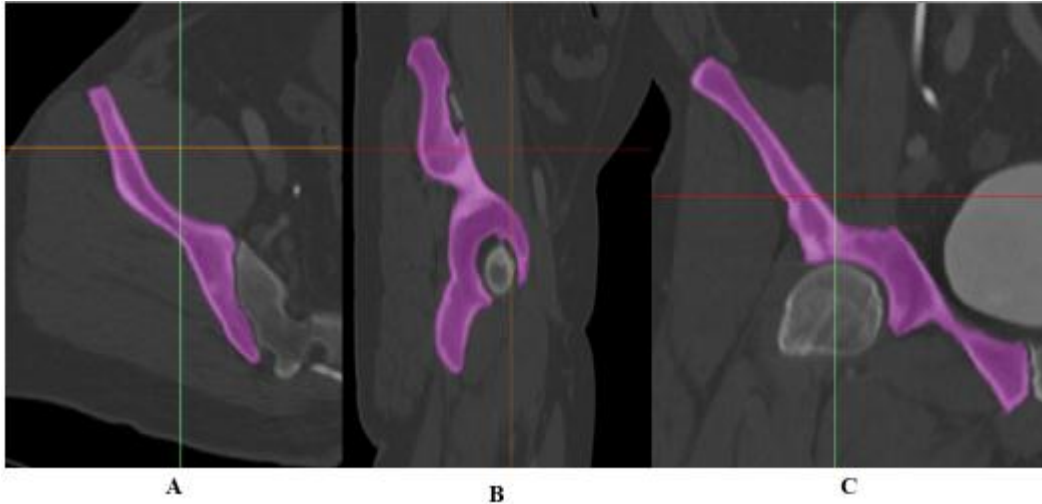


Figure 3.6 (c) Pelvis after Split Mask Function

Views, A. Coronal view, B. Axial view, C. Sagittal view

The femur bone was segmented into (i) cortical bone Figure 3.7 (a) ; (ii) cancellous bone Figure 3.7 (b) by Mimics Innovation suite 19. A Boolean intersection operation was performed between cortical bone and pelvis so that a realistic model was created for loading conditions.



Figure 3.7(a) Cortical Bone 2D

Views. A. Coronal view, B. Axial view, C. Sagittal view

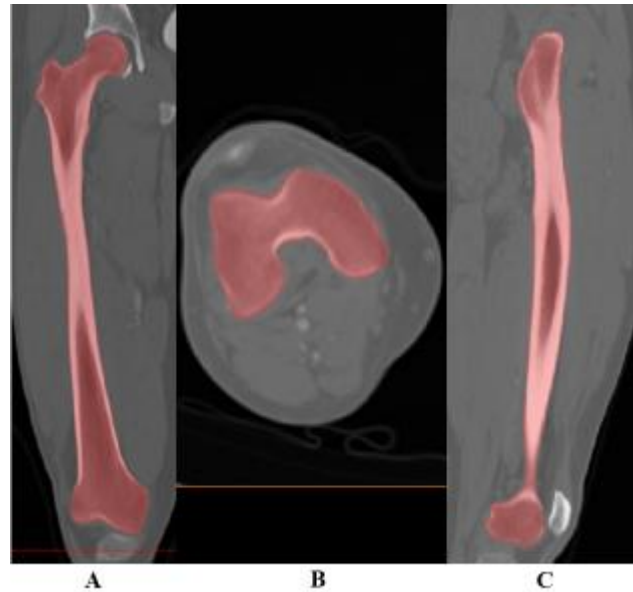


Figure 3.7 (b) Cancellous Bone 2D,

Views; A. Coronal view, B. Axial view, C. Sagittal view

In Mimics Innovation Suite, a 3D model with multiple structures is constructed as a non-manifold assembly. The non-manifold assembly forms common surface between different masks to achieve good quality mesh. For example cortical bone with trabeculae bone, these geometries are known as non-manifold assemblies typically contains two or more volumes sharing common surface.

3.4 3-Matic For Mesh generation

3-Matic is 3D modeling program which enables to create, optimize and modify meshes using CAD designs or scanned data for finite element analysis. While running FE analysis on multiple parts it is important to create link between different layers, for this purpose non-manifold assembly is created.

In creation of non-manifold assembly the order in which masks were placed is of prime importance as explained in Chapter 4 ,section 4.3. Figure 3.8 presents different stages of non-manifold assembly. Once non-manifold assembly (Figure 3.8 A) is formed, smooth and reduce functions were applied (Figure 3.8, B, C) and then volume mesh with tetrahedral elements was formed (Figure 3.8 D). The assembly was then copied to mimics for material

properties assignment (Figure 3.8 F). After material properties assignment, models were exported as input deck files for finite element analysis in a numerical solver Abaqus CAE.

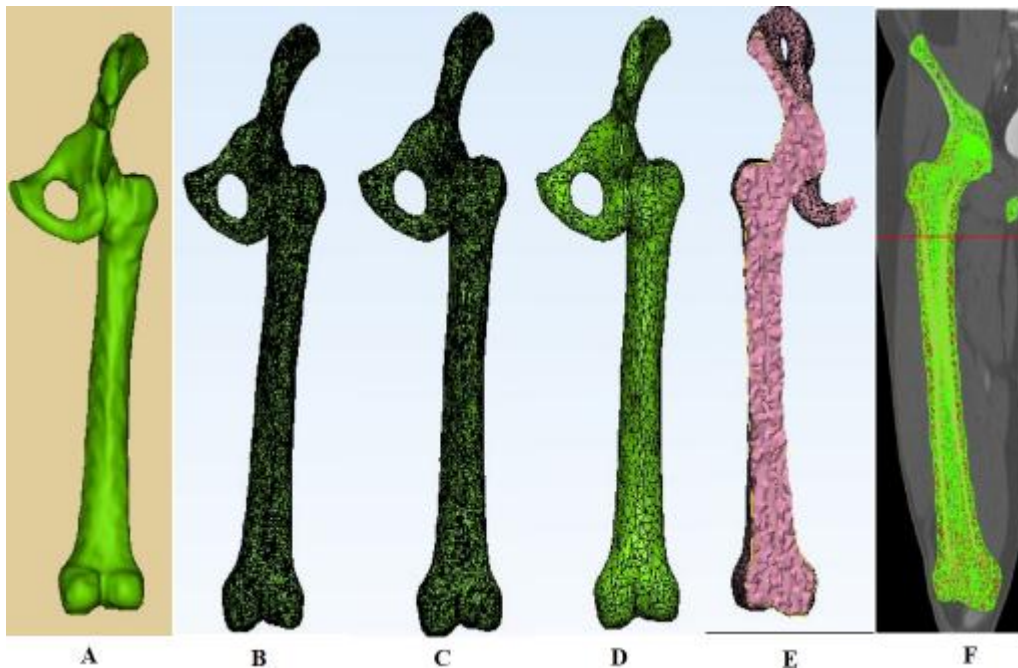


Figure 3.8 Non-manifold Assembly Formation for Mesh Generation, A. Non-manifold Assembly, B. Non-manifold Assembly after smooth function application, C. Non-manifold Assembly after Reduce function application, D. Volume Mesh generation, E. Internal view of volume elements, F. Material Properties assignment

3.5 Healthy and Diseased Models

To create healthy and necrotic models for finite element analysis; same dataset was used. Firstly, healthy models were created from dataset with varying mesh densities. Additionally, necrosis is virtually induced in the same dataset using data from the literature as bench mark. The process of generating healthy models is same as explained in **section 3.3 and 3.4**.

The diseased models were created by manually editing healthy data set using the benchmark dataset (Beaulé and Amstutz, 2004). Random slices were edited for the induction of necrosis. For reference guide, a scheme representing different stages of necrosis was followed as established in the literature (figure 3.9). As femoral necrosis is present in femur head so the actual site of disease progression is not universal and varies from patient to patient.



Figure 3.9 Scheme of Stages of Avascular Femoral Necrosis Adapted for the Project Adapted from Management of Ficat Stage III and IV Osteonecrosis of the Hip, Beaulé PE, Amstutz HC, J Am Acad Orthop Surg. 2004;12(2):96–105

3.5.1 Diseased Models Generation

To create diseased models, scheme presented in figure 3.9 was followed. The diseased models were presented in figure 3.10(A) Stage I, figure 3.10(B) Stage II, figure 3.10(C) Stage III, figure 3.10(D) Stage IV. Different color scheme represent different mask which were edited manually to create four stages of AVN. The color scheme adopted is explained in figure legends and dotted area presents the area from where pixels were deleted for diseased models creation.

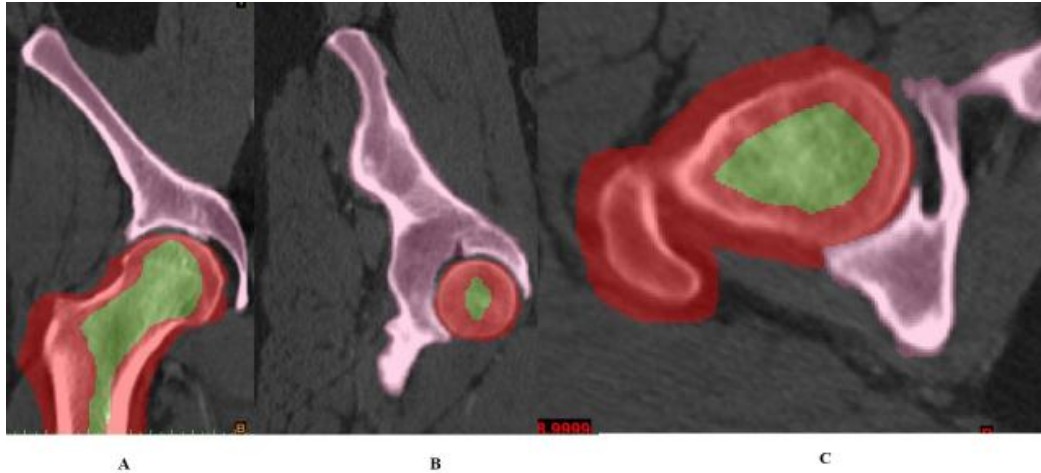


Figure 3.10(A) Satges of AVN:Stage I, Views A. Sagittal view, B. Coronal view,C. Axial view , Color Scheme:,Pink =Pelvis, Red=Cortical bone, Green=Cancellous bone

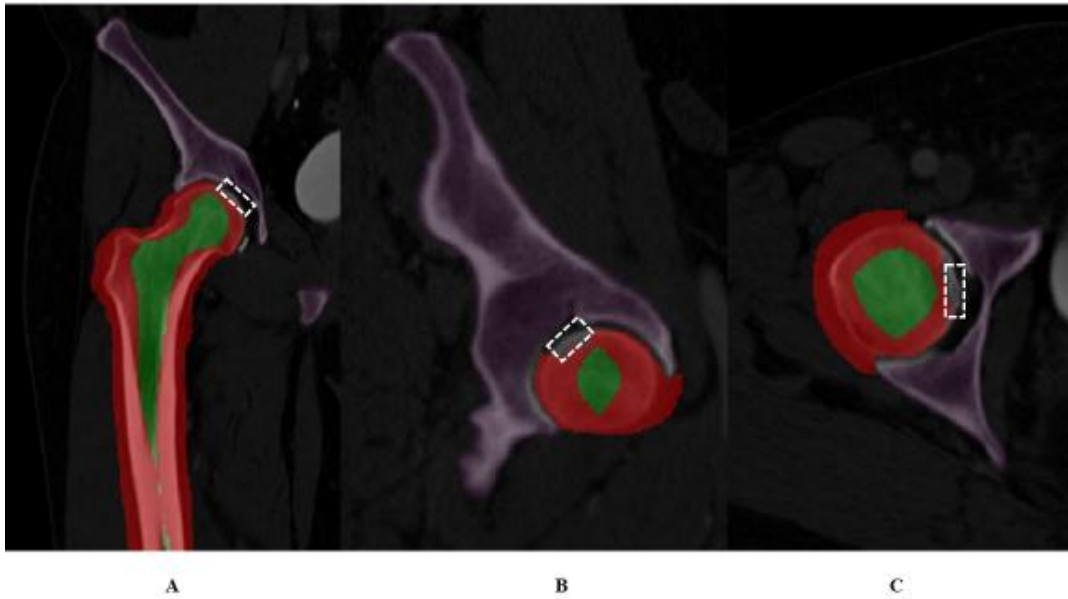


Figure 3.10(B) Satges of AVN:Stage II, Views A. Sagittal view, B. Coronal view, C. Axial view,Color Scheme: Pink =Pelvis, Red=Cortical bone, Green=Cancellous bone

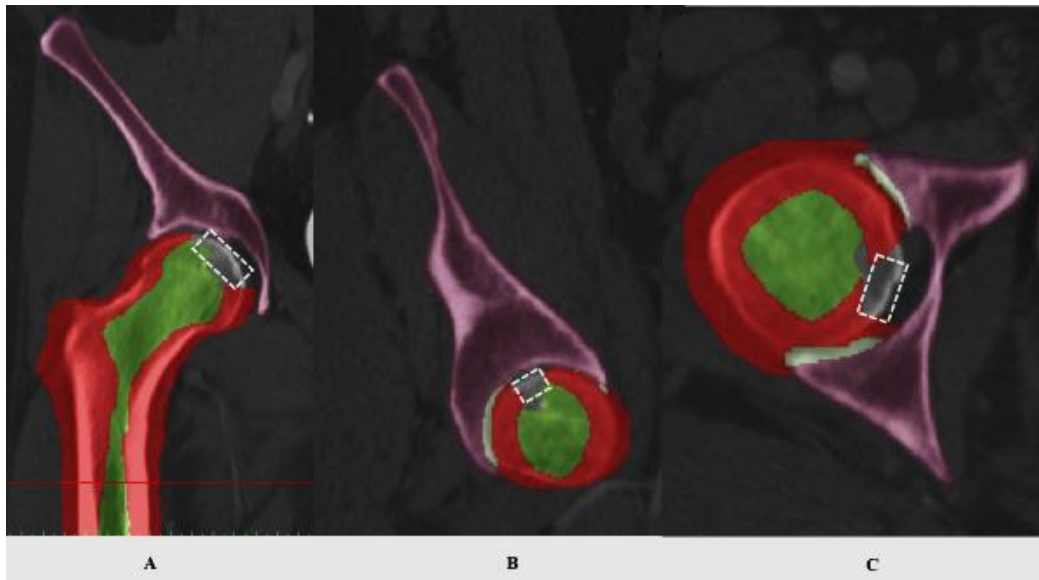


Figure 3.10(C) Stages of AVN: Stage III; Views A. Sagittal view, B. Coronal view, C. Axial view, Color Scheme: Pink =Pelvis, Red=Cortical bone, Green=Cancellous bone

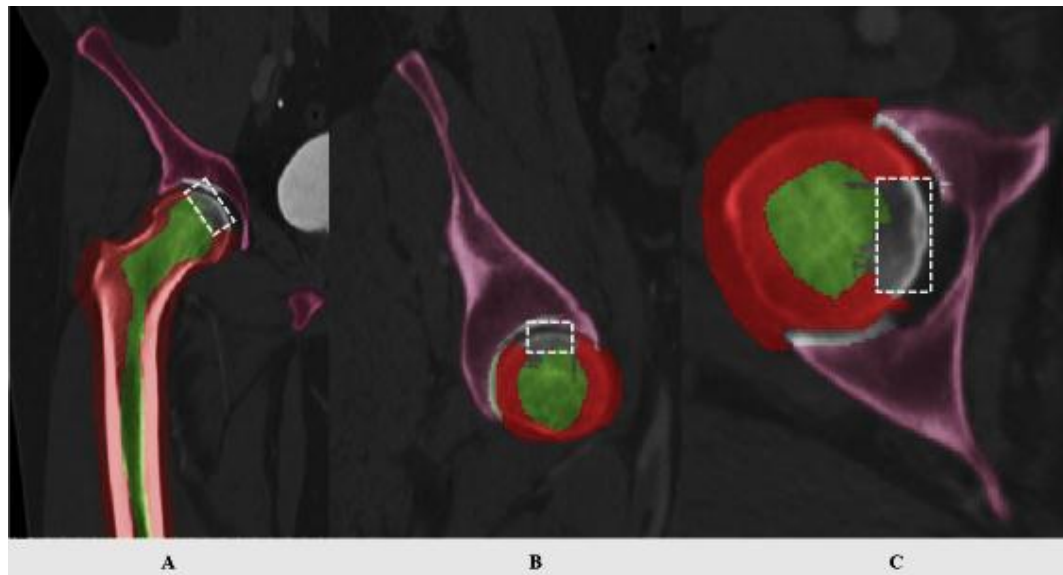


Figure 3.10(D) Stages of AVN :Stage IV, Views: A. Sagittal view, B. Coronal view, C. Axial view, Color Scheme: Pink =Pelvis, Red=Cortical bone, Green=Cancellous bone

3.6 Numerical Modeling using FEA

Computational models of joints anatomy and function provide a means for bio mechanist, physician, and physical therapist to understand the effect of repetitive motion, acute injury, and degenerative diseases. Furthermore, such models may be used to improve design of prosthetic implant (Mackerle, 2006).

In early 1970's finite element analysis found its application to find out stresses in bone biomechanics. Later, finite element modeling becomes most promising technique to develop subject/patient specific models in a rapid and reliable manner. Among the existing methods, FEA is most widely used because of its ability to represent complex geometries and anatomical features. It gives insight of the structure being analyzed and often is the only choice where physical examination is not feasible (Reznikov et al., 2014). Once models are formed by the 3-mtaic and tetrahedral mesh with C3D4 type elements are formed, then models are imported to a numerical solver Abaqus for analysis.

3.6.1 Boundary Conditions

As small change in boundary conditions can lead to erroneous results, boundary conditions therefore play a great role. The choice of boundary condition depends upon the type of analysis. For FE analysis of femur bone attached with pelvis the BC used are, femur bone is fixed at the distal end such that it cannot translate or rotate in any direction. For this purpose, **ENCASTER** boundary condition was used Figure 3.11. Mathematically ENCASTER boundary conditions is presented as

$U1 = U2 = U3 = UR1 = UR2 = UR3 = 0$, where U represents displacement and R represents rotation. This means that proximal end of femur bone is not allowed to displacing or rotating in any x, y and z direction. This type of BC is utilized for natural loading conditions.

The type of load applied on the surface present between the pelvis and cortical bone is **Surface Traction** at an angle in X direction. In surface traction a vector is chose for load application. This load is transferred to head of the femur from pelvis and then to shaft Figure 3.11.

The load applied calculated by equation
*Force = Mass of the body * acceleration due to gravity* (1)

$$F = 50Kg * 9.8 ms^{-2}$$

$$F = 490N$$

To calculate nodal force which is applied on chosen vector the formula is

$$Nodal\ Force = \frac{Total\ Force}{No.\ of\ nodes}$$

$$Nodal\ Force = \frac{490N}{3} = 163N$$

This nodal force is applied on the chosen vector at an angle in X direction so that force is exerted in the same direction to ensure natural loading condition.

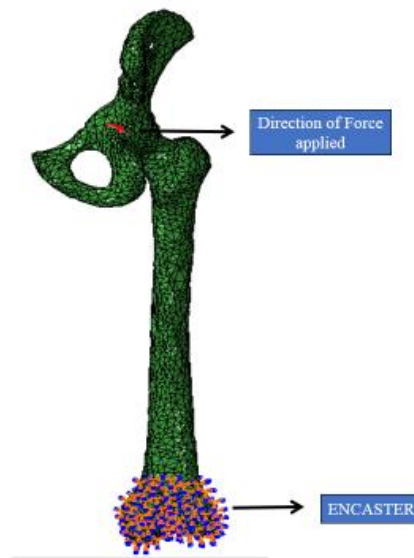


Figure 3.11 Boundary Conditions

The material properties are second most important part of FE analysis. The material properties which are used in this analysis are given in the Table 3.2.

	Young's Modulus (MPa)	Poisson Ratio	Reference
Cortical Bone	22500	0.33	(Lai et al., 2015)
Cancellous Bone	13500	0.33	(Lai et al., 2015)
Pelvis	2875	0.29	(Hao et al., 2011)
Necrotic Bone	124.6	0.152	(Zhou et al., 2014)

Table 3.2 Material Properties Utilized in the analysis

3.6.2 Convergence Analysis

Often it is asked whether results obtain from finite elements analysis are valid or not? For this purpose, convergence test is done. For most of the linear problems iterative methods are not required yet mesh convergence is important for linear problems. Convergence analysis is when by changing the number of elements in the mesh; solution for that mesh does not change and becomes constant. Then the results are said to be converged. For convergence analysis four coarseness levels are attain by changing edge lengths from Model 1 to Model 4 which are presented in Table 3.3. The model A has lowest mesh coarseness level where as model D has finer mesh.

Models	Mesh Densities
Model A	18,986
Model B	38,318
Model C	57,176
Model D	76,527

Table 3.3 Mesh Densities for Convergence Analysis

3.7 Comparison of Results

In computational work it is quite important to validate results by some mathematical model. But in some cases the geometries are complex and to develop a mathematical is quite difficult task. So in order to verify results of the simulations are compared with literature. If simulation results follow the same trend as available in literature then results are said to be true for that scenario.

In this research we have created a model of femur with intact pelvis, for which a mathematical model can be archived but that would not explain the real geometry. In order to validate this study we have conducted literature search and found a reference study to compare our results with it.

Chapter 4

Results

Overview

This chapter critically discusses results obtained from this study. The chapter further reviews limitations and discussion on acquired results. The chapter is divided into following sections:

1. Results from Scanning (Computed Tomography)
2. Results obtained from image processing.
3. Results obtained from finite element analysis
4. Validation

4.1 Results from Scanning

The results from whole body micro computed tomography scan were acquired on 16 CT scanner to create 2D images as shown Figure 4.1. The image specification was presented in Chapter 3 table 3.1.

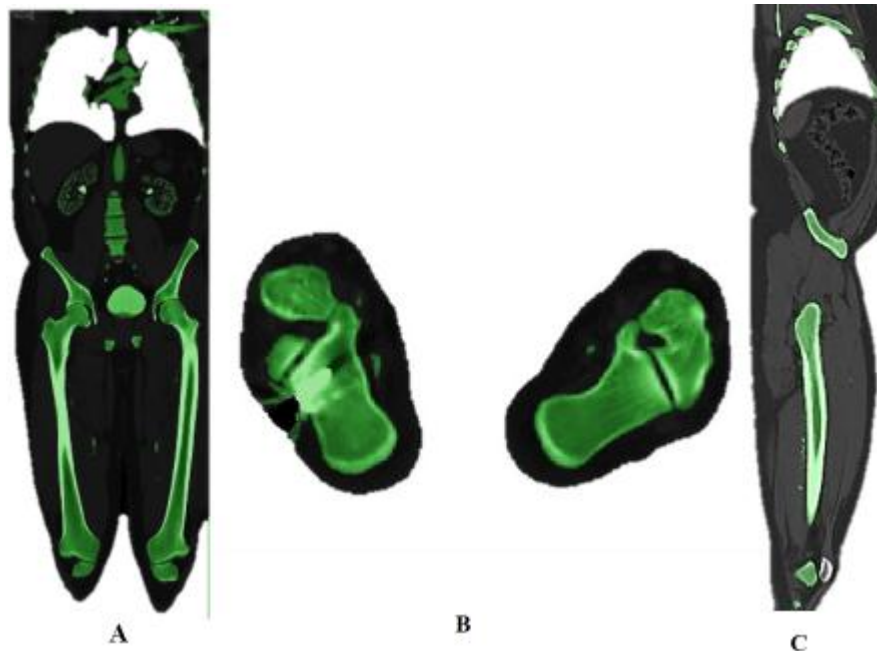


Figure 4.1 2-D presentation of dataset, A. Sagittal View, B. Axial View, C. Coronal View

4.2 Results from Image Processing using Mimics Innovation Suite

After image segmentation, whole body scan Figure 4.2(A) was obtained. Since whole-body scan was not required for the study so region of interest was cropped out i.e. pelvis attached with femur bone Figure 4.2(B). Due to time constrains and computational cost only right femur attached with pelvis was used for image base modeling in this study (Refer Figure 4.2 (C)).



Figure 4.2 Image Processing Results

A. Whole Body Scan, B. Segmented ROI, C. Femur attached with Pelvis

After the required ROI was segmented out, femur and pelvis were separated by split mask function and assigned distinctive masks. In Figure 4.3 femurs was presented with pink mask whereas pelvis was presented by blue mask. After split mask function was performed femur was assigned blue mask and pelvis purple mask as presented in Figure 4.3.

Femur bone is the strongest, largest bone and bears around one fifth of the total weight of human body. It is segmented out into two distinctive parts (i) Cortical Figure 4.4 (A) bone and (ii) Cancellous bone Figure 4.4 (B) by Boolean operation and Figure 4.4 (C) show outer cortical and inner cancellous bone in high transparency.

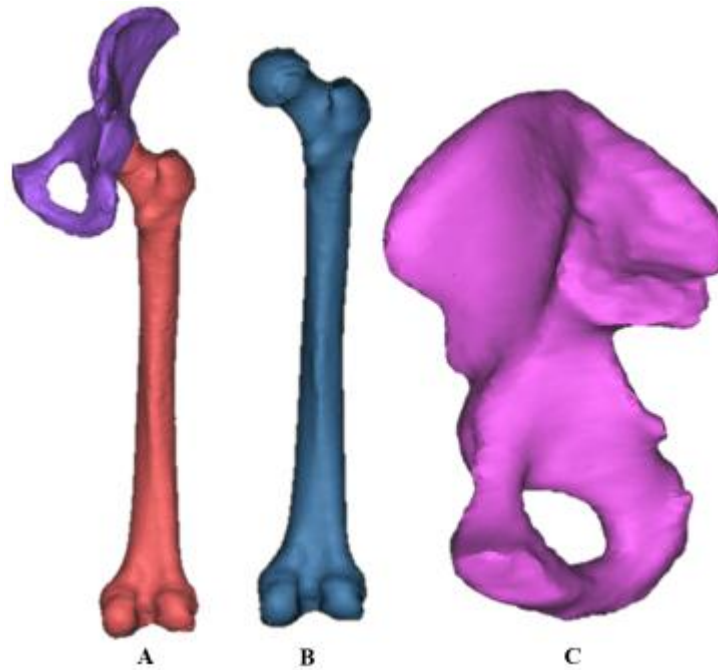


Figure 4.3 Image Processing Results

Split Mask Function: A. femur pink mask and pelvis in purple mask, B. Femur, C. Pelvis

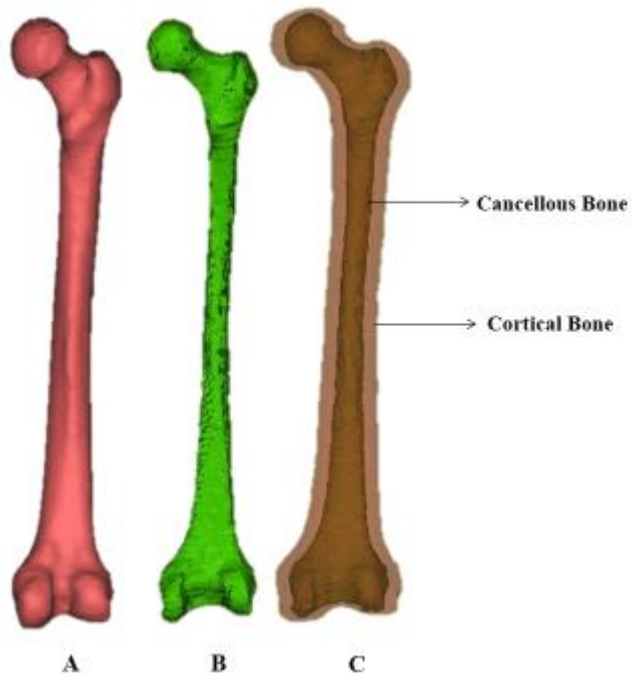


Figure 4.4 Cortical and Cancellous bone Presentation in 3D A. Cortical Bone, B. Cancellous Bone, C. Outer Cortical and inner Cancellous Bone in 3D

4.2.1 3-Matic Results

As explained in the Chapter 3 section 3.5 - 3-Matic forms non-manifold assembly. This is presented in the figure 4.5 (A). The orders in which masks are present in non-manifold assembly are;

1. Pelvis
2. Intersecting mask between the pelvis and cortical bone
3. Cortical bone mask
4. Cancellous bone mask, figure 4.5 (B).

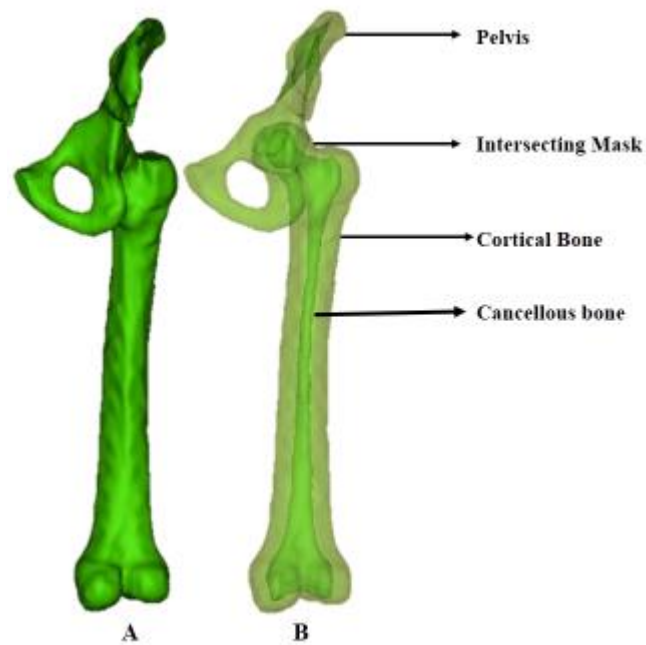


Figure 4.5 3-Matic Results

A.Non-manifold Assembly, B. Non-manifold Assembly in high transparency showing internal msk

4.2.2 Results for Healthy Models

Once non-manifold assembly is formed four healthy models with varying edge length were generated for finite element analysis. In figure 4.6, (A) Model 1 represents first mesh with lowest elements, whereas in figure 4.6 (B) model 2 represent mesh with increased elements. In this way model 3 figure 4.6 (C) and model 4 figure 4.6 (D) were generated. Models 4 have highest mesh density.

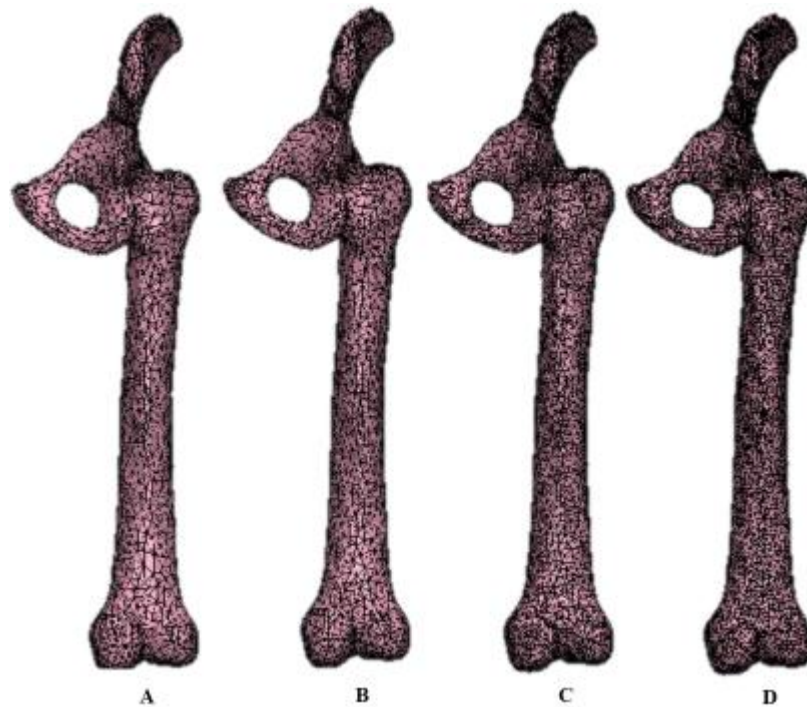


Figure 4.6 Four Healthy Models with increasing mesh densities from Model A- D, Mesh Densities Presented in Chapter 3, Table 3.2

4.2.3 Results for AVN Models

In figure 4.7 four AVN models were presented according to stage of the disease. These models were created by following the scheme presented in chapter 3; section 3.6. The black color in figure 4.7 represents diseased area.

Table 4.1 presents four stages of AVN along with mesh densities. The first stage of AVN has highest number of elements and number of elements decreased in second stage.

Whereas in third and fourth stage of necrosis number of elements were increased. This increase in number of element could be due to large interfaces in geometrical details and as disease progresses empty places were created in the models.

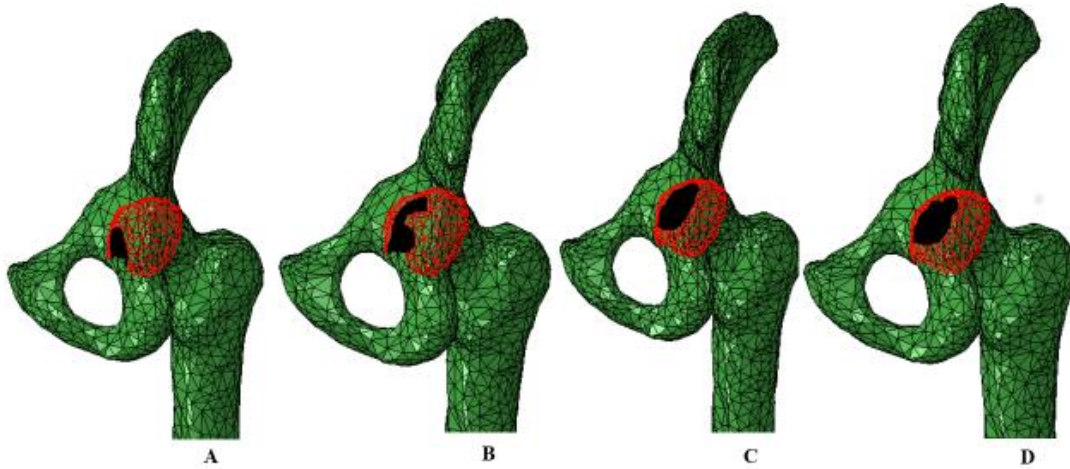


Figure 4.7 Stages of AVN, Black color presents diseased area

A. Stage I, B. Stage II, C. Stage III, D. Stage IV

AVN Models Mesh Densities	
Stage of AVN	Number of Mesh Elements
Stage I	89,863
Stage II	53,172
Stage III	1,12681
Stage IV	1,42915

Table 4.1 Stages of AVN Models with Mesh Densities

4.3 Results from Finite Element Analysis

Finite element analysis is the most common computational technique used to study biomechanical function of bone. The advancement in imaging modalities and wide spread use of FEM provides a strong impulse for bone research to understand complex nature of bone and to develop patient specific models. Below the results from FEM analysis are explained, which are obtained from this research.

4.3.1 Convergence Analysis

In Finite element analysis, convergence analysis is often required to verify results. Convergence analysis is the iterative method in which results are converged to a solution and become independent of mesh size.

For this study four models were created for convergence test. Models were created with increasing mesh densities as presented in figure 4.6. The results obtained from convergence analysis are explained in the following paragraph.

In figure 4.8 a graph between displacement and mesh densities is plotted. The mesh densities for models A-D were present on x-axis and displacement on y-axis. Mesh densities and respective displacements are presented in table 4.2. Model A has lowest mesh density of 18,986 elements and has displacement of 0.062mm. The second model has displacement of 0.02mm; with increase in the mesh density from model C to D we achieved a constant displacement which is 0.01mm. At this point results are said to be converged and become independent of mesh size

Mesh Density	Displacement (mm)
18,986	0.062 mm
38,378	0.02mm
57,176	0.01 mm
76,524	0.01 mm

Table 4.2 Mesh Densities vs. Displacement for Converged Models

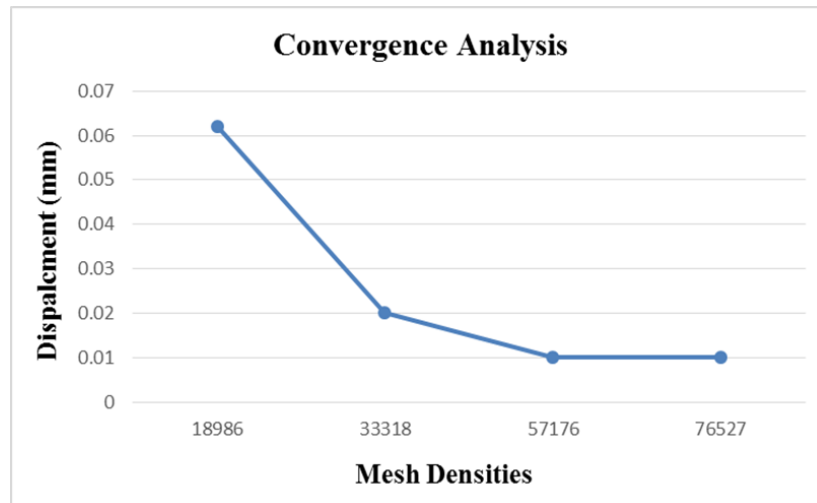


Figure 4.8 Analyses for Deformation

In figure 4.9, graph of Mises stress in relation with mesh density is plotted. According to FEA theory, accuracy of FEM results depends upon mesh density (element size) and computational time. Models with fine mesh density (small elements size) yield more accurate results as compared to results obtained from coarser mesh densities (large element size) (Liu and Glass, 2013). This is because; denser elements tend to have more saturated distribution for stress as well as pressure. Models with fine mesh densities give accurate results and take more computational time as compared to results from coarser meshes. In finer meshes there are more elements to compute thus yield accurate results. It can be seen from the graph that with the increase in mesh density Mises stress decreases. Model A has highest Mises Stress (113 MPa) which is significantly reduced from model B to model D (45MPa). Although overall, the models are not converged perfectly, however they are going towards finer stress numbers which means they will converge after one or two more iteration. The reason why, we could not run more models were due to the computational limitation of our system. In future, it will be possible to have run more models and get more accurate results.

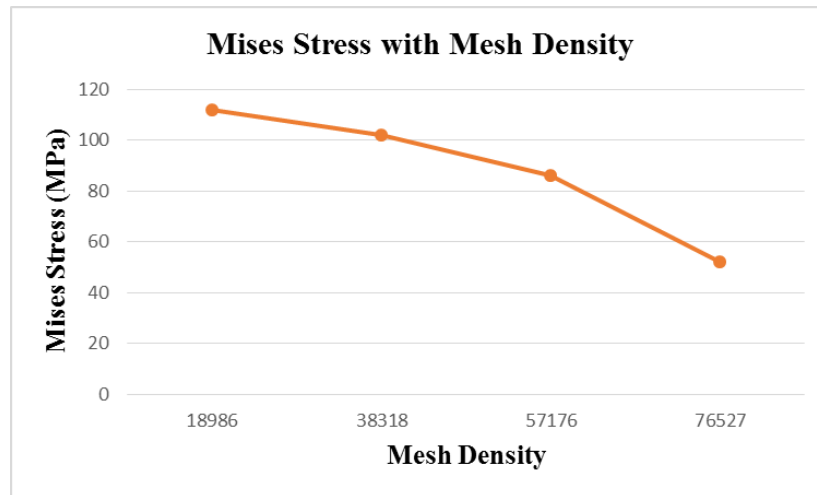


Figure 4.9 Mises Stress Analysis with increasing mesh density

4.3.2 Results from Healthy Models

Results from healthy models with varying mesh densities were obtained using Abaqus CAE by applying boundary conditions and material properties assignment exactly in the similar was as in the diseased models. Four coarseness levels were defined for healthy models. A constant surface traction was applied on a chosen vector for all models.

A set of deformation and Mises Stress are shown in the Figure 4.10 and Figure 4.11 for four converged healthy models under same loading conditions.

Figure 4.10 shows deformation contours in healthy models from A to D for four converged models. The minimum deformation noted is 0.062mm. Values used for contours are very much same as for models from A to D. Model B has deformation of 0.02mm which decreases to 0.01mm for model D. At this point displacements were converged.

Figure 4.11 shows contour of Mises stress in healthy models. The maximum value of Mises Stress obtained for this study was 113MPa as compared to yield stress (180-200MPa) of bone. This stress is in bone safety limit as reported in literature.

In figure 4.11 it is seen that much of the stress is concentrated in shaft region. The shaft region has ability to withstand compressional loads than other tensile loads (Einhorn, 1992). More over shaft is considered to be solid in this study. Maximum Von-Mises stress values obtained for this study was 113MPa for Model A with highest mesh density. This

stress is in safety region of bone as reported in literature which is 180-200 MPa (Reilly and Burstein, 1975, Izwan et al., 2012, Biewener, 1993).

Mechanically femur bone is adapted to bear compressive forces. The arrangement of cortical and cancellous bone in femur is of advantage, these bears compressive forces to prevent bending moment in bone (Rudman et al., 2006). Structurally shaft of femur bone is the weak part and is prone to fracture at high stresses.

In this study bone is considered to be solid and mathematically stress distribution in solid bone is directly related to the measure of moment of inertia I . The moment of inertia is defined as "the area of moment of inertia across the natural axis of bone/beam". The moment of inertia for the solid cylinder is given as

$$I = \frac{\pi r^4}{4} \dots\dots\dots (6)$$

The moment of inertia is the measures of resistance to the bending and it depends upon the cross sectional area and radius of cylinder (Whiting and Zernicke, 2008).

In literature values reported for the strength of bone are in the range of 180-200 MPa, the model under study is femur bone which is long bone and bears most of the body weight. The maximum stress seen in this study is 113 MPa towards the lower condyle in is concentrated in shaft region. This shows that femur shaft is weak part of bone and cannot bear higher stress. Naturally humans are bipedal and have strong femur to provide stability to core.

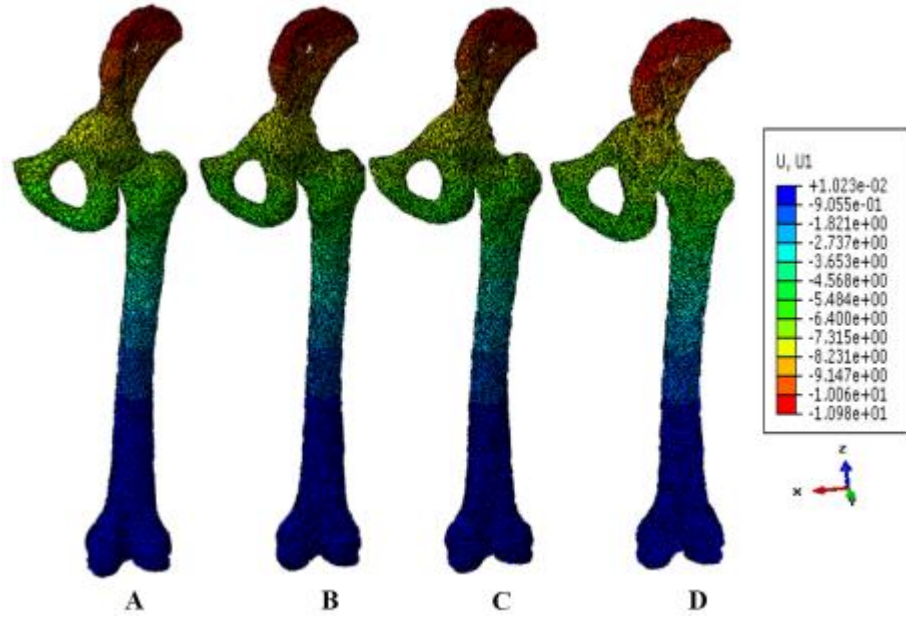


Figure 4.10 Plot of Deformation in Healthy Models from Model A-D

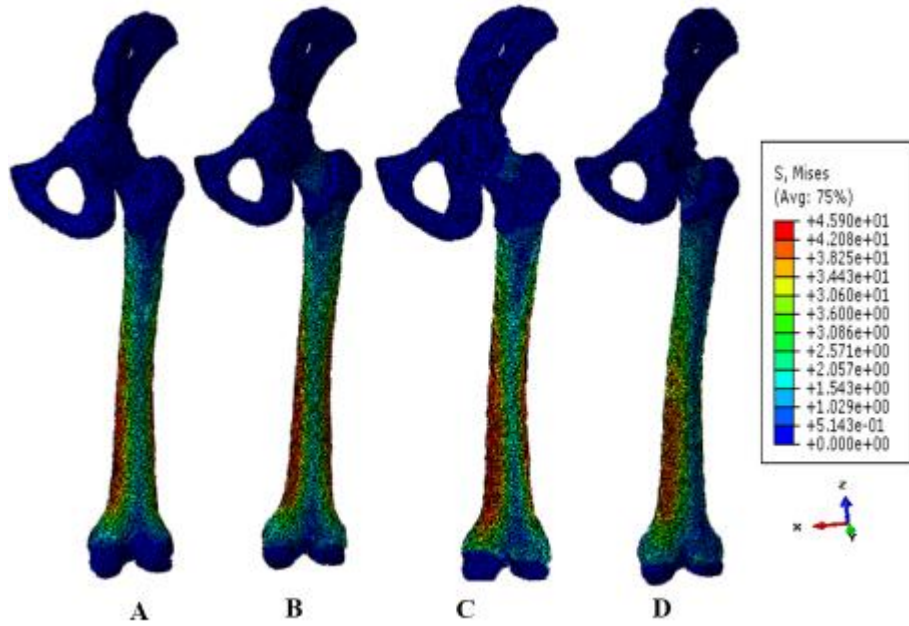


Figure 4.11 Plot of Mises Stress Distribution in Healthy Models from A-D

4.3.4 Results of AVN Models

In this section, FE analysis of AVN models is presented according to the stage of the disease. One of the aims of this thesis was to develop models of different stages of AVN to investigate effect of different necrotic lesion sizes.

For the AVN models same boundary conditions were applied but material properties of necrotic tissue were employed. A constant surface traction force was applied on the chosen vector. The results obtained after the Abaqus CAE are discussed below in detail.

Four different models were generated according to the stage of the disease, the number of mesh elements depend upon the stage of the disease. The stage I has the 89,863 number of elements then in the second stage II the number of elements decreases to 53,172 but in the third and fourth stage of disease the number of elements increases. The mesh densities according to the stage of the disease are presented in Table 4.1.

The deformation and Mises Stress plots of AVN models are presented in the figure 4.12 and 4.12 respectively. It can be clearly seen form the figures that with the increase in stage of disease deformation and Mises Stress increases. The maximum deformation and Mises Stress is seen the Stage IV which is 0.04mm and 163MPa respectively.

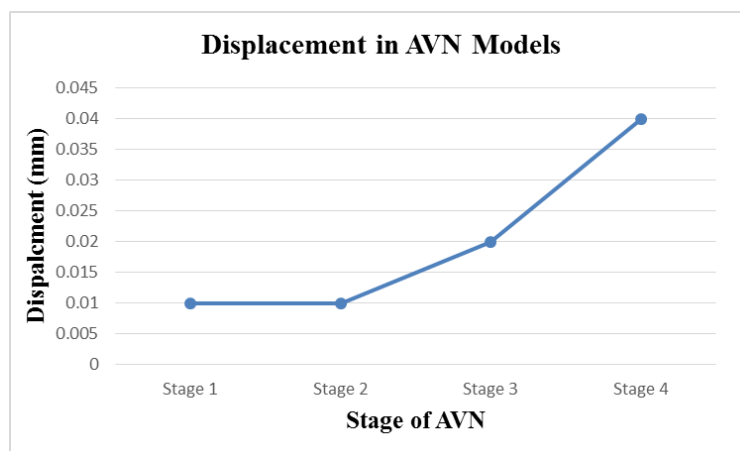


Figure 4.12 Deformation w.r.t Stages of AVN

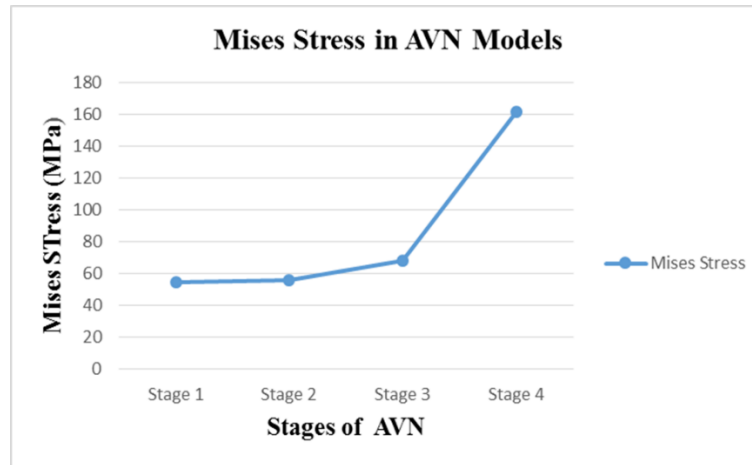


Figure 4.13 Mises Stress w.r.t Stages of AVN

In Figure 4.14 and 4.15 the plot of deformation and Mises Stress are presented w.r.t the stages of AVN. It can be seen from the figures that with the increase in the stage of disease deformation and Mises Stress increased and maximum deformation is seen in stage IV of AVN. The stress distribution in the models depend upon certain factors such as the magnitude and direction of load, material properties and the physical connections between environment (Anderson, 2015).

Due to necrosis internal structure of healthy and necrotic bone is different (Zhou et al., 2014), therefore their material properties are different as well. This change in material properties will affect mechanical strength of bone (Anderson, 2015). From the results it is seen that with the increase in the stage of disease stress pattern were different and highest Mises Stress was seen in stage IV of AVN.

The stress distribution in structure depends upon certain factors such as geometry of bone, load applied and material properties. According to Wolf's bone adapt to the load applied. The minimum stress was seen in the Stage I (55MPa), this was because during initial stage of disease bone tries to remodel itself and distribute load according to new bone geometry, which results in less stress.

The maximum stress from FE analysis of AVN was seen in Stage IV 163 MPa and deformation was 0.04mm. This Mises Stress is concentrated in the neck region of the femur bone, the site where bone structure is lost. There are two important factors in the determination of the stress distribution

- Size
- Location of the necrotic lesion.

Lesion size is important for identifying stage of the disease. Lesions can vary in size, location and frequency (Shahi Avadi, 2016). In this study, Ficat classification was followed; according to which if more than 30% femur head is damage is considered as stage IV AVN. In literature different studies are reported to study effect of lesion size and reported that when more than 30% head is damage then femur head would collapse. At this stage only choice of treatment available is hip replacement therapy, to provide support and stability to core.

Finite element studies showed that cancellous bone play important role in support and strength of cortical bone. During necrosis cancellous bone lost its structure in femur head as a result cortical bone losses its mechanical strength and bend (Chen et al., 2017, Zhou et al., 2014).

This may be due the reason and also reported in literature stress is concentrated at the necrotic site. This changes the internal microstructure of cortical and cancellous bone. Bone also try to remodel itself at necrotic region to redistribute stress locally (Chen et al., 2017).

In the present study necrotic area is described as material with decreases elastic modulus. According to the Wolf's law bone adjust to the mechanical environment (Chen et al., 2015). In case of necrosis; bone adapt to change in material properties and try to remold itself so distribute load. But this remodeling process is slow, this results in the increases stresses at the necrotic region.

Today most of the FE studies focus volume of necrosis on impact of damage progression. FE results showed that the stress centered at the necrotic site. This localization of stress could be function of many parameters, including traumatic incidents, mechanical environment and slippage event(Wen et al., 2017).

The internal view of the femur bone shows the stress distribution in the head and neck. Maximum stress was seen in the head and neck region, which eventually travels down to shaft and forms an evident pattern of stress.

In Figure 4.16 stress pattern of the articulating surface is presented. The main trend is that as the stage of the necrosis increases, stress pattern increases due to loss of bone structure. However, in our study, stage III is a bit exaggerated in terms of an abnormal stress pattern. This could be perhaps because of the singularity or mesh error as well. Pelvis forms a ball and socket type of joint with femur head and reduces friction but disease condition the frictional forces came into play and may degrade the cartilage. This results in increased stresses at the attachment site. Maximum Mises Stress is present in the stage IV which (43 MPa).

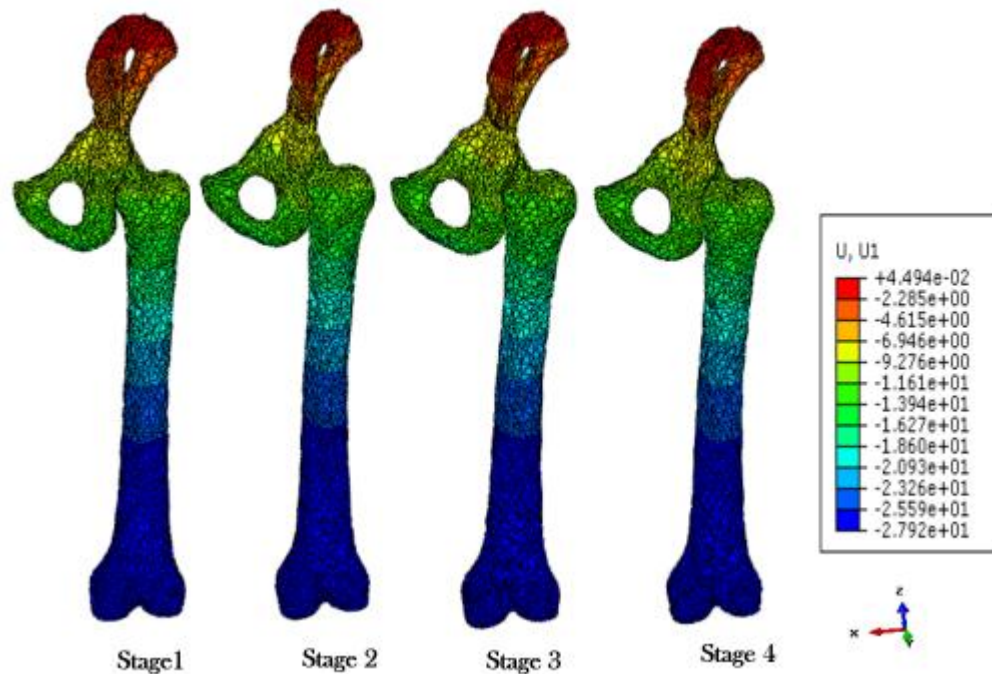


Figure 4.14 Plots of Deformation w.r.t stages of AVN

Stage I, B. Stage II, C. Stage III, C. Stage

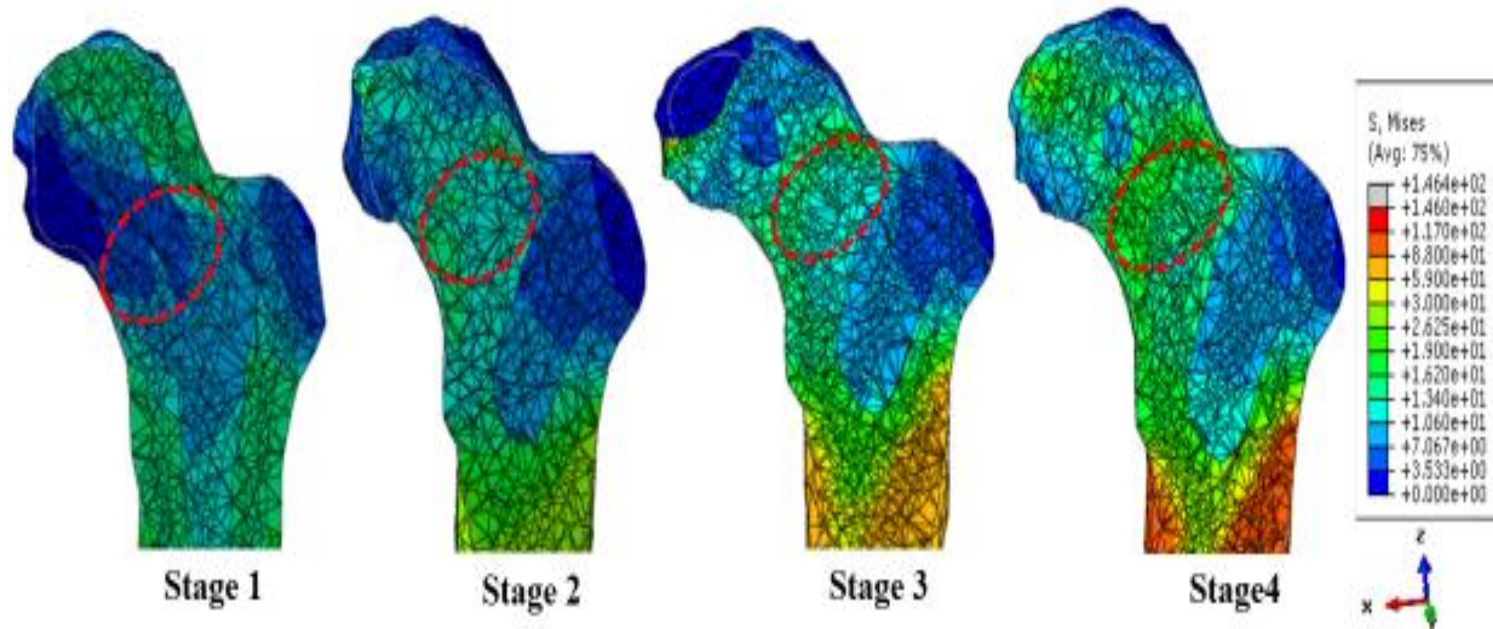


Figure 4.15 Misses Stress Distribution w.r.t Stage of AVN

A. Stage I, B. Stage II, C. Stage III, D. Stage

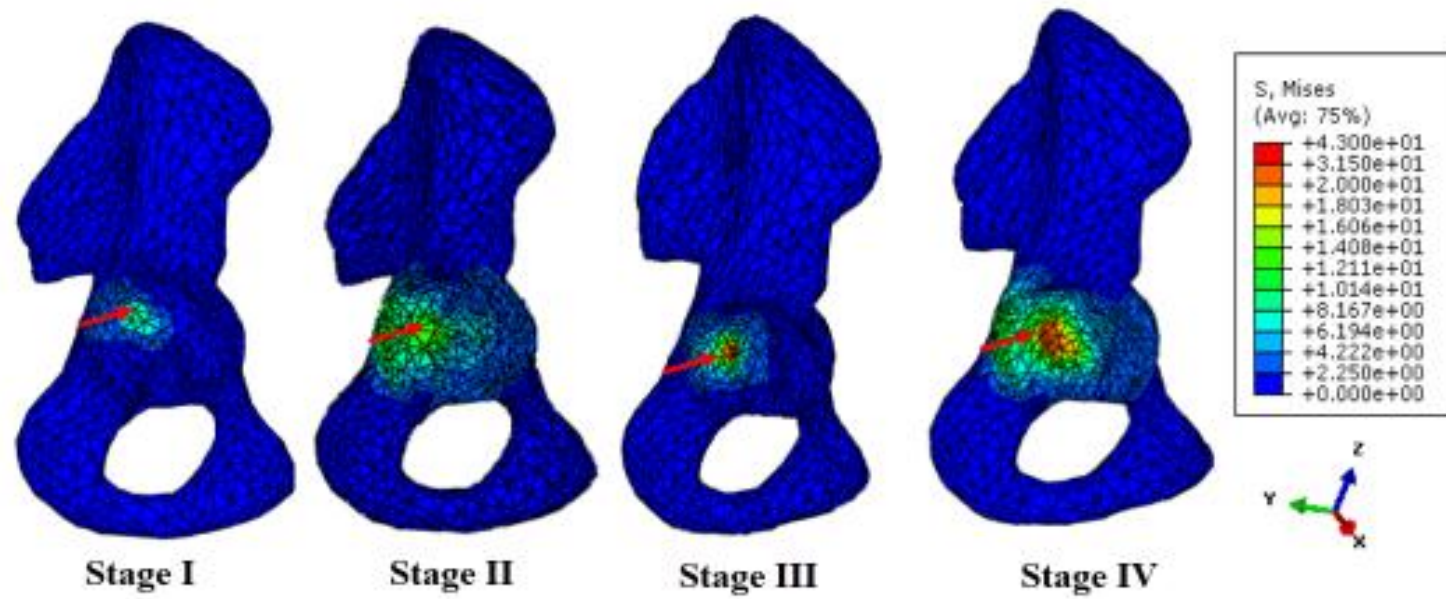


Figure 4.16 Stress at Articulation Points on Pelvis

4.3.5 Effect of Weight on AVN Models

Here FE analysis under different loading conditions have been presented for different body weights. For this purpose four models were generated according to the stage of the AVN but with varying body weight. The bone is subjected to the same loading and boundary conditions but force applied is different and calculated by the following equation

$$F = \text{body weight} * \text{gravity}$$

$$F = 50 * 9.8 = 490 \text{ N}$$

$$\text{Nodal Force} = \frac{\text{Total Force}}{\text{No. of Nodes}} = \frac{490}{3} = 163 \text{ N}$$

Where m varies from 50-80 Kg and for each case a different nodal force is calculated according to body weight as presented in Table 4.3.

AVN Models	
Weight (Kg)	Force (N)
50 Kg	163.33 N
60 Kg	196 N
70 Kg	228.6 N
80 Kg	261.3 N

Table 4.3 Force Calculation w.r.t Body Weight

The results which were obtained after FEA analysis are represented below. It can be seen from Figure 4.17 and Figure 4.18 that with the increase in body weight deformation and Mises stress also increases. The maximum deformation and Mises Stress is observed for the stage IV for 80Kg body weight.

In the Figure 4.17 there is similar trend seen in case of displacement pattern at stage I and stage II, but Mises Stress distribution is quite different. The difference is may be due to reason at early stage of necrosis bone try to bear stress and redistribute load internally and thus preventing it from large displacement but Mises Stress shows increasing trend. In this study the pattern maybe showing not the similar trend as we try to induce manually which

may be depict the internal stress pattern as in case of real bone damage. But overall results present the similar pattern. At stage IV with maximum body weight maximum stresses and displacement were observed Mises stress exceeds bone safety. This result in the permanent increases in stress as bone can no longer in the elastic limit to withstand stress.

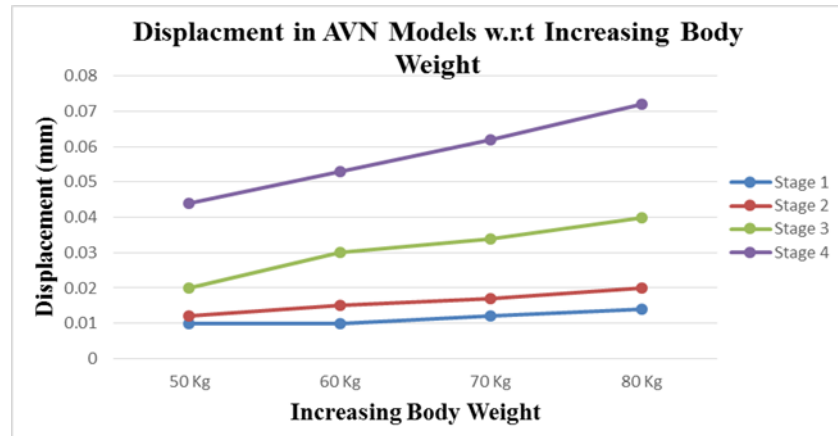


Figure 4.17 Displacement w.r.t Increasing Body Weight

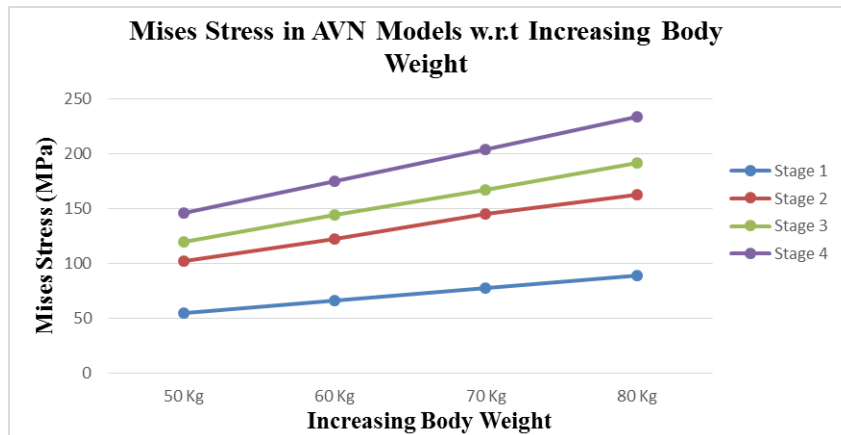


Figure 4.18 Mises Stress w.r.t Increasing Body Weight

4.4 Comparison of Results from Literature

FE analysis were validated by comparing the simulated results obtained with the already data available in literature. In this study intact hip surface with different stages of necrosis was subjected under same loading conditions but with different material properties.

Although simulated results were validated by mathematical modeling but in case of complex bone geometries it is sometime difficult to acquire mathematical solution which

cannot explain the complex geometry so the results were compared with already data available for model validation.

For the present study femur bone intact with pelvis was conducted and results after FE analysis were subjected to be compared with already available literature. In literature different studies are conducted to study the effect of necrotic lesion size on the stress distribution. As stress distribution in the diseased area would help not only in prognosis but also for treatment options. The results of the present study were compared with results from literature and it was found out the stress pattern observed in the FE results were quite consistent with available literature.

Experimental Models	Mises Stress (MPa)	Literature Models	Mises Stress (MPa)	Reference
Stage I	5			(Chen et al., 2015)
Stage II	19	Model (10mm degradation)	12.5	
Stage III	23.5	Model B (20mm degradation)	17.8	
Stage IV	26.5	Model D (30mm degradation)	26.78	

Table 4.4 Validation of Results from Literature

4.5 Comparison of Results of Healthy and AVN Models

Healthy and AVN model results were compared in order to get a clear picture of how stresses and displacement travel in both models. In healthy model stresses were less concentrated in the neck region as compared to the AVN models. The healthy femur bone head is able to withstand more compressive strains because of the bone architecture.

In AVN models corresponding regions of femoral neck was utilized to calculate stress and strain. As the damage progresses to later stage, stress increases in the head and neck of the femur bone. Since AVN is the disease of femur head so it's the ultimate site for stress and strain progression. The size of the necrotic lesion plays important role in the stress distribution pattern as well as the lesion location. This would lead to abnormal stress concentration and stress distribution in the femur head and ultimately femur head would fall off losing its functional support.

In table 4.5 comparisons of the healthy converged models is presented with different stage of AVN. As Table shows that with the increases in the stage displacement and Mises Stress increases.

Comparison of Healthy and AVN Models				
Healthy Model		AVN Models		
Mises Stress (MPa)	Displacement (mm)	AVN Model	Mises Stress (MPa)	Displacement (mm)
3.6 MPa Healthy Converged Model	0.01mm Healthy Converged Model	S1	5	0.01
		S2	19	0.01
		S3	23.5	0.02
		S4	26.50	0.04

Table 4.4 Comparison of Results of Healthy and AVN Models

The localized stress from both the healthy and AVN models were compared from the same region. There is an increasing trend that was observed that with the increase in the stage of

the disease localized stress also followed the same trend. The neck of the femur bone in the event of AVN experiences compressive loads

The stress and the contact distribution pattern in the healthy and necrotic bone is different. Healthy bone has tendency to bear more compressive loads because of the cortical and cancellous bone architecture. Cortical bone has the capacity to bear compressive loads and provide support to femur bone. Whereas in case of AVN bone micro architecture is lost and load distribution becomes uneven thus bone fail to bear loads and stress is concentrated in the femur head and neck. In our full model bone shaft bear excessive stress at the distal end of the joint.

Chapter 5

Discussion

In this research we have created healthy and necrotic models to study stresses and strains under normal physiological loads. This study is particularly designed to investigate stresses encountered by the necrotic models under normal body functioning the event of disease progression. The physical models were constructed using image processing and finite element analysis.

Both healthy and necrotic bone show stress and deformation pattern. However stresses are much higher in the necrotic regions as compared to the healthy ones. These stresses travel down to shaft and makes it vulnerable to fracture, since shaft is the weakest structure in the femur, yet bears a lot of load and moments. This damage and behavior could be related to the changes in the mechanical properties of necrotic bone as compared to healthy bone (for example 41% change in ultimate tensile strength and 51% reduction in elastic modulus) (Anderson, 2015). There is evidence that stiffness and strength is reduced 72% and 51 % respectively after necrosis in the femur bone (Shahi Avadi, 2016).

Our results at necrotic region show that the where there is the geometrical curvature stresses are the function of the bone degradation location of necrosis in neck. In calculating localized Misses Stress from same location of healthy and necrotic bone it came out that as disease progresses to later stages stress is increased in the head and neck region of the bone which eventually travels down to the shaft. We infer that there is no short cut to the treatment of necrosis however correct diagnosis is required before a logical treatment is planned. Wrong measure may lead to traumatic dislocation of the hip and slipping of the upper femoral epiphysis

From literature it is observed that stress and deformation in necrotic models depends upon number of factors, some of which are size and location of the necrotic area respectively, application and direction of load on cortical and cancellous bone structure.

The pattern of the stress in healthy and necrotic femur bone play important role in the bone strength. Presence of the different size lesion in case of AVN results in altered stress

transfer which causes region of higher stress. Furthermore change in the mechanical properties of bone also results in higher stresses.

Literature to date reported a lot of data on elastic behavior relative to elastic beam theory. Larger the curvature of the beam larger the bending moments. In our full model of femur bone apart from the femur neck shaft did not experiences larger bending moments due to small curvature. Moreover, if we apply Euler's Bernoulli equation to our analysis since bone is analogous to a beam; we will get quite similar results as in the classic beam mechanics.

Chapter 6

Future Work and Limitation

FEA is the most reliable tool for biomechanical analysis. Though approximated, but there is no other way to test the intricate geometries except testing them physically. Some compromises are made in this research are

- AN Online dataset was used whereas ideally patient specific dataset should be used for analysis.
- For the FE analysis, static body weights were used whereas ideally other forces such as muscle forces, ground reaction forces should also be considered.
- Only static- elastic analysis was performed in this analysis, which might not be very accurate yet would serve as a starting point for dynamic analysis

REFERENCES

REFERENCES

- AMANATULLAH, D. F., STRAUSS, E. J. & DI CESARE, P. E. 2011. Current management options for osteonecrosis of the femoral head: part 1, diagnosis and nonoperative management. *Am J Orthop (Belle Mead NJ)*, 40, E186-92.
- ANDERSON, J. A. 2015. *In vitro and in silico simulations of femoral heads with avascular necrosis*. University of Leeds.
- ASNIS, S. E. & WANKE-SGAGLIONE, L. 1994. Intracapsular fractures of the femoral neck. Results of cannulated screw fixation. *JBJS*, 76, 1793-1803.
- ASSOULINE-DAYAN, Y., CHANG, C., GREENSPAN, A., SHOENFELD, Y. & GERSHWIN, M. E. Pathogenesis and natural history of osteonecrosis. *Seminars in arthritis and rheumatism*, 2002. Elsevier, 94-124.
- ASSOULINE-DAYAN, Y., CHANG, C., GREENSPAN, A., SHOENFELD, Y., GERSHWIN. 2002. *RE: Pathogenesis and natural history of osteonecrosis. Seminars in Arthritis and Rheumatism*.
- BACHILLER, F. G.-C., CABALLER, A. P. & PORTAL, L. F. 2002. Avascular necrosis of the femoral head after femoral neck fracture. *Clinical orthopaedics and related research*, 399, 87-109.
- BARRACK, R. L. 1999. Symptomatic multifocal osteonecrosis: a multicenter study. *Clinical orthopaedics and related research*, 312-326.
- BEAULÉ, P. E. & AMSTUTZ, H. C. 2004. Management of Ficat stage III and IV osteonecrosis of the hip. *JAAOS-Journal of the American Academy of Orthopaedic Surgeons*, 12, 96-105.
- BENIASH, E. 2011. Biominerals—hierarchical nanocomposites: the example of bone. *Wiley Interdisciplinary Reviews: Nanomedicine and Nanobiotechnology*, 3, 47-69.
- BIEWENER, A. A. 1993. Safety factors in bone strength. *Calcified Tissue International*, 53, S68-S74.
- BYRNE, D. P., MULHALL, K. J. & BAKER, J. F. 2010. Anatomy & biomechanics of the hip. *The open sports medicine Journal*, 4.
- CHEN, L., HONG, G., FANG, B., ZHOU, G., HAN, X., GUAN, T. & HE, W. 2017. Predicting the collapse of the femoral head due to osteonecrosis: From basic methods to application prospects. *Journal of Orthopaedic Translation*, 11, 62-72.
- CHEN, W.-M. 2011. Osteonecrosis of the femoral head: Surgical perspective. *Formosan Journal of Surgery*, 44, 131-135.
- CHEN, Z., XU, Y., QI, Z. & ZHO, J. 2015. The formation and function of the sclerosis rim in the femoral head: A biomechanical point of view. *Medical engineering & physics*, 37, 1125-1132.
- CHIU, K., SHEN, W., TSUI, H. & CHAN, K. 1997. Experience with primary exeter total hip arthroplasty in patients with small femurs: review at average follow-up period of 6 years. *The Journal of arthroplasty*, 12, 267-272.
- CHIU, K. H., SHEN, W. Y., CHEUNG, K. W. & TSUI, H. F. 2005. Primary Exeter total hip arthroplasty in patients with small femurs: a minimal of 10 years follow-up. *The Journal of arthroplasty*, 20, 275-281.
- CHOI, H.-R., STEINBERG, M. E. & CHENG, E. Y. 2015. Osteonecrosis of the femoral head: diagnosis and classification systems. *Current reviews in musculoskeletal medicine*, 8, 210-220.
- COOPER, C., STEINBUCH, M., STEVENSON, R., MIDAY, R. & WATTS, N. 2010. The epidemiology of osteonecrosis: findings from the GPRD and THIN databases in the UK. *Osteoporosis international*, 21, 569-577.
- CURREY, J. D. 2002. *Bones: structure and mechanics*, Princeton university press.

REFERENCES

- DANIEL, M., HERMAN, S., DOLINAR, D., IGLIC, A., SOCHOR, M. & KRALJ-IGLIC, V. 2006. Contact stress in hips with osteonecrosis of the femoral head. *Clinical orthopaedics and related research*, 447, 92-99.
- EHLINGER, M., MOSER, T., ADAM, P., BIERRY, G., GANGI, A., DE MATHELIN, M. & BONNOMET, F. 2011. Early prediction of femoral head avascular necrosis following neck fracture. *Orthopaedics & Traumatology: Surgery & Research*, 97, 79-88.
- EINHORN, T. A. 1992. Bone strength: the bottom line. *Calcified tissue international*, 51, 333-339.
- FUKUSHIMA, W., FUJIOKA, M., KUBO, T., TAMAKOSHI, A., NAGAI, M. & HIROTA, Y. 2010. Nationwide epidemiologic survey of idiopathic osteonecrosis of the femoral head. *Clinical Orthopaedics and Related Research*®, 468, 2715-2724.
- GARELLICK, G., KÄRRHOLM, J., ROGMARK, C. & HERBERTS, P. 2009. Swedish Hip Arthroplasty Register: Annual Report, 2008. *Department of Orthopaedics, Sahlgrenska University Hospital*.
- GAUTIER, E., GANZ, K., KRÜGEL, N., GILL, T. & GANZ, R. 2000. Anatomy of the medial femoral circumflex artery and its surgical implications. *Bone & Joint Journal*, 82, 679-683.
- GRAY, H. 1878. *Anatomy of the human body*, Lea & Febiger.
- HAO, Z., WAN, C., GAO, X. & JI, T. 2011. The effect of boundary condition on the biomechanics of a human pelvic joint under an axial compressive load: a three-dimensional finite element model. *Journal of biomechanical engineering*, 133, 101006.
- HEAD, M. J. & BARR, A. 2013. Orthopaedics 3. The proximal limbs. *Equine medicine, surgery and reproduction 2nd ed. Philadelphia: Elsevier*, 369-388.
- HOLMBERG, S. & DALEN, N. 1987. Intracapsular pressure and caput circulation in nondisplaced femoral neck fractures. *Clinical orthopaedics and related research*, 219, 124-126.
- HOUGAARD, K. & THOMSEN, P. 1986. Traumatic posterior dislocation of the hip—prognostic factors influencing the incidence of avascular necrosis of the femoral head. *Archives of orthopaedic and traumatic surgery*, 106, 32-35.
- IZWAN, S., RAZAK, A., FADZLIANA, N., SHARIF, A., AIZAN, W. & RAHMAN, W. A. 2012. Biodegradable polymers and their bone applications: a review.
- JERGESEN, H. E., HELLER, M. & GENANT, H. K. 1990. Signal variability in magnetic resonance imaging of femoral head osteonecrosis. *Clinical orthopaedics and related research*, 253, 137-149.
- JONES JR, J. P. & PELTIER, L. F. 2001. Alcoholism, Hypercortisonism, Fat Embolism and Osseous Avascular Necrosis. *Clinical orthopaedics and related research*, 393, 4-12.
- KANG, J. S., PARK, S., SONG, J. H., JUNG, Y. Y., CHO, M. R. & RHYU, K. H. 2009. Prevalence of osteonecrosis of the femoral head: a nationwide epidemiologic analysis in Korea. *The Journal of arthroplasty*, 24, 1178-1183.
- KAUSHIK, A. P., DAS, A. & CUI, Q. 2012. Osteonecrosis of the femoral head: an update in year 2012. *World journal of orthopedics*, 3, 49.
- LABEK, G., THALER, M., JANDA, W., AGREITER, M. & STÖCKL, B. 2011. Revision rates after total joint replacement. *J Bone Joint Surg Br*, 93, 293-297.
- LAI, Y.-S., CHEN, W.-C., HUANG, C.-H., CHENG, C.-K., CHAN, K.-K. & CHANG, T.-K. 2015. The effect of graft strength on knee laxity and graft in-situ forces after posterior cruciate ligament reconstruction. *PloS one*, 10, e0127293.
- LAI, Y.-S., WEI, H.-W. & CHENG, C.-K. 2008. Incidence of hip replacement among national health insurance enrollees in Taiwan. *Journal of orthopaedic surgery and research*, 3, 42.
- LIEBERMAN, J. R. 2004. Core decompression for osteonecrosis of the hip. *Clinical orthopaedics and related research*, 418, 29-33.

REFERENCES

- LIU, Y.-F., CHEN, W.-M., LIN, Y.-F., YANG, R.-C., LIN, M.-W., LI, L.-H., CHANG, Y.-H., JOU, Y.-S., LIN, P.-Y. & SU, J.-S. 2005. Type II collagen gene variants and inherited osteonecrosis of the femoral head. *New England Journal of Medicine*, 352, 2294-2301.
- LIU, Y. & GLASS, G. 2013. Effects of Mesh Density on Finite Element Analysis. SAE Technical Paper.
- LOIZOU, C. & PARKER, M. 2009. Avascular necrosis after internal fixation of intracapsular hip fractures; a study of the outcome for 1023 patients. *Injury*, 40, 1143-1146.
- LU-YAO, G. L., KELLER, R. B., LITTENBERG, B. & WENNERBERG, J. E. 2005. Outcomes after displaced fractures of the femoral neck. A meta-analysis of one hundred and six published reports. *Orthopedic Trauma Directions*, 3, 29-33.
- LV, H., DE VLAS, S. J., LIU, W., WANG, T. B., CAO, Z. Y., LI, C. P., CAO, W. C. & RICHARDUS, J. H. 2009. Avascular osteonecrosis after treatment of SARS: a 3-year longitudinal study. *Tropical Medicine & International Health*, 14, 79-84.
- MA, J.-X., HE, W.-W., ZHAO, J., KUANG, M.-J., BAI, H.-H., SUN, L., LU, B., TIAN, A.-X., WANG, Y. & DONG, B.-C. 2017. Bone Microarchitecture and Biomechanics of the Necrotic Femoral Head. *Scientific reports*, 7, 13345.
- MACKERLE, J. 2006. Finite element modeling and simulations in orthopedics: a bibliography 1998–2005. *Computer methods in biomechanics and biomedical engineering*, 9, 149-199.
- MALIZOS, K. N., KARANTANAS, A. H., VARITIMIDIS, S. E., DAILIANA, Z. H., BARGIOTAS, K. & MARIS, T. 2007. Osteonecrosis of the femoral head: etiology, imaging and treatment. *European journal of radiology*, 63, 16-28.
- MARANGALOU, J. H. 2013. Patient specific prediction of bone failure using microstructure-enhanced continuum finite element models.
- MARIEB, E. N. & SMITH, L. A. 2003. *Human Anatomy and Physiology Laboratory Manual: Cat Version*, San Francisco.
- MITCHELL, M., KUNDEL, H., STEINBERG, M., KRESSEL, H., ALAVI, A. & AXEL, L. 1986. Avascular necrosis of the hip: comparison of MR, CT, and scintigraphy. *American Journal of Roentgenology*, 147, 67-71.
- MIYAMOTO, Y., MATSUDA, T., KITO, H., HAGA, N., OHASHI, H., NISHIMURA, G. & IKEGAWA, S. 2007. A recurrent mutation in type II collagen gene causes Legg-Calve-Perthes disease in a Japanese family. *Human genetics*, 121, 625-629.
- MOYA-ANGELER, J., GIANAKOS, A. L., VILLA, J. C., NI, A. & LANE, J. M. 2015. Current concepts on osteonecrosis of the femoral head. *World journal of orthopedics*, 6, 590.
- MUSTANSAR, Z. 2015. *Selection of modelling level of detail for incorporating stress analysis into evolutionary robotics simulations of extinct and extant vertebrates*. University of Manchester.
- ORBAN, H. B., CRISTESCU, V. & DRAGUSANU, M. 2009. Avascular necrosis of the femoral head. *MAEDICA-a Journal of Clinical Medicine*, 4, 26-34.
- PAPPAS, J. N. 2000. The musculoskeletal crescent sign. *Radiology*, 217, 213-214.
- REILLY, D. T. & BURSTEIN, A. H. 1975. The elastic and ultimate properties of compact bone tissue. *Journal of biomechanics*, 8, 393-397.
- REZNIKOV, N., SHAHAR, R. & WEINER, S. 2014. Bone hierarchical structure in three dimensions. *Acta biomaterialia*, 10, 3815-3826.
- RHO, J.-Y., KUHN-SPEARING, L. & ZIOUPOS, P. 1998. Mechanical properties and the hierarchical structure of bone. *Medical engineering & physics*, 20, 92-102.
- RUDMAN, K., ASPDEN, R. M. & MEAKIN, J. R. 2006. Compression or tension? The stress distribution in the proximal femur. *Biomedical engineering online*, 5, 12.
- RUFFONI, D. & VAN LENTHE, G. 2017. 3.10 Finite Element Analysis in Bone Research: A Computational Method Relating Structure to Mechanical Function☆.

REFERENCES

- SABAH, S., HENCKEL, J., COOK, E., WHITTAKER, R., HOTH, H., PAPPAS, Y., BLUNN, G., SKINNER, J. & HART, A. 2015. Validation of primary metal-on-metal hip arthroplasties on the National Joint Registry for England, Wales and Northern Ireland using data from the London Implant Retrieval Centre: a study using the NJR dataset. *The bone & joint journal*, 97, 10.
- SAINI, A. & SAIFUDDIN, A. 2004. MRI of osteonecrosis. *Clinical radiology*, 59, 1079-1093.
- SHAHI AVADI, M. 2016. *Characterisation and Development of an Experimental Mechanical Model of Avascular Necrosis of the Femoral Head*. University of Leeds.
- SMITH, F. B. 1959. Effects of Rotatory and Valgus Malpositions on Blood Supply to the Femoral Head: Observations at Arthroplasty. *JBJS*, 41, 800-815.
- TSAI, S.-W., WU, P.-K., CHEN, C.-F., CHIANG, C.-C., HUANG, C.-K., CHEN, T.-H., LIU, C.-L. & CHEN, W.-M. 2016. Etiologies and outcome of osteonecrosis of the femoral head: Etiology and outcome study in a Taiwan population. *Journal of the Chinese Medical Association*, 79, 39-45.
- WEINER, S. & WAGNER, H. D. 1998. The material bone: structure-mechanical function relations. *Annual Review of Materials Science*, 28, 271-298.
- WEN, P.-F., GUO, W.-S., ZHANG, Q.-D., GAO, F.-Q., YUE, J.-A., LIU, Z.-H., CHENG, L.-M. & LI, Z.-R. 2017. Significance of lateral pillar in osteonecrosis of femoral head: a finite element analysis. *Chinese medical journal*, 130, 2569.
- WHITING, W. C. & ZERNICKE, R. F. 2008. *Biomechanics of musculoskeletal injury*, Human Kinetics.
- ZHOU, G.-Q., PANG, Z.-H., CHEN, Q.-Q., HE, W., CHEN, Z.-Q., CHEN, L.-L. & LI, Z.-Q. 2014. Reconstruction of the biomechanical transfer path of femoral head necrosis: A subject-specific finite element investigation. *Computers in biology and medicine*, 52, 96-101.